THE ADSORPTION OF SULFUR DIOXIDE ON ACTIVATED CARBONS FROM PEANUT HULLS AND WASTE RUBBER

A THESIS

Presented to

The Faculty of the Division

of Graduate Studies

By

John Allen Hatfield

In Partial Fulfillment

of the Requirements for the Degree

Master of Science in Chemical Engineering

Georgia Institute of Technology

June, 1976

THE ADSORPTION OF SULFUR DIOXIDE ON ACTIVATED CARBONS FROM PEANUT HULLS AND WASTE RUBBER

Approved:

William R. Ernst, Chairman

Clyde Orr, Jr.

Waldemar T. Ziegler

Date approved by Chairman: 8/2/70

ACKNOWLEDGMENTS

The author wishes gratefully to acknowledge his advisor, Dr. William R. Ernst, of the Chemical Engineering Department, and reading committee members, Dr. Clyde Orr, Jr. and Dr. Waldemar T. Ziegler, for their guidance. Appreciation is also extended to Dr. Anthony Hines for the help he gave throughout this project.

The financial support of the Environmental Protection Agency has also been deeply appreciated.

TABLE OF CONTENTS

LIST OF TABLES

LIST OF ILLUSTRATIONS

NOMENCLATURE

A_X	cross-sectional area of bed (cm^2)
b	radius of particle (cm)
C_o'	inlet concentration of sulfur dioxide (ppm)
C_o	inlet concentration of sulfur dioxide (gm/cm^3)
c(L,t)	effluent concentration of sulfur dioxide (gm/cm^3)
D	intraparticle diffusivity (cm^2/sec)
F	volumetric flow rate (cm^3/min)
G	volumetric flow rate corrected to 491.67°R and 1 atm (cm^3/min)
h	fluid film coefficient (cm/sec)
K_D	equilibrium coefficient (dimensionless)
m	void volume/particle volume
P	barometric pressure (mm Hg)
q	average sulfur dioxide concentration on the adsorbent (gm/cm^3)
q_i	sulfur dioxide concentration at a particular point in the adsorbent particle (gm/cm^3)
R	gas constant (cm^3 mm Hg/gm-mole-°R)
R_f	film resistance (sec)
R_e	Reynolds number for a packed bed (dimensionless)
r	radial coordinate in the particle (cm)
T	bath temperature (°R)
t	time elapsed from the start of the run (min)
V_B	total volume of the bed (cm^3)

V_p	volume of particles in the bed (cm^3)
v	linear flowrate (cm/sec)
W	weight of the bed (gm)
Y	adsorbate contact time (dimensionless)
z	distance from the inlet (cm)
ε	bed void fraction (dimensionless)
x	Rosen parameter ($3K_D LD/mvb^2$)
ν	Rosen parameter (mvR_f/L)
ρ_b	bulk density of adsorption medium (gm/cm^3)
ρ_p	particle density (gm/cm^3)
τ	length of time of run (min)
θ	t-z/v (sec)
μ	viscosity of gas at the inlet (gm/cm-sec)

SUMMARY

This investigation was undertaken in order to evaluate sulfur dioxide adsorption by activated carbons produced from waste materials. The two materials chosen and evaluated were waste rubber obtained from a tire retreading operation and peanut hulls. Two commercially available activated carbons were evaluated in similar fashion as a comparison. These were Nuchar from Westvaco and activated charcoal from Barnebey Cheney.

The gas compositions used for study were 951 ppm, 5005 ppm, and 11,278 ppm sulfur dioxide in nitrogen. The other variables, temperature, flowrate, pressure, and particle diameter were held constant at 78°F, 300 cm^3/min, 745 mm Hg, and 4.745×10^{-2} cm, respectively.

Of the materials tested, activated carbon produced from peanut hulls was the most effective adsorbent for sulfur dioxide. It was found that this carbon possessed a high equilibrium adsorption capacity, exhibited a very steep breakthrough curve, and was less dense than the commercial carbons used. Intraparticle diffusivities ranging from 4.46×10^{-6} cm^2/sec to 7.45×10^{-5} cm^2/sec and equilibrium coefficients, K_D, ranging from 2767 to 7560 were found for the activated carbon derived from peanut hulls.

Waste rubber did not prove to be as effective as

peanut hull carbon as indicated by its lower equilibrium coefficient. These values were generally less than 2482. For comparison, the Nuchar from Westvaco had intraparticle diffusivities ranging from 1.05×10^{-6} cm^2/sec to 3.23×10^{-6} cm/sec and K_D values ranging from 2448 to 4663.

The experiments were conducted by passing a carrier gas, nitrogen, containing SO_2 through a fixed bed of activated carbon. The breakthrough curves were measured as a function of time and fitted to Rosen's general solutions for fixed bed adsorption. Equilibrium coefficients were determined by numerically integrating the breakthrough curves and the sample intraparticle diffusivities were determined from Rosen's solutions.

CHAPTER I

INTRODUCTION

The problem of air pollution is becoming generally recognized, and desulfurization of flue gas by means of adsorption is being more fully examined. The major problems accompanying stack gas cleaning are: (1) large quantities of gas are involved, (2) low concentrations of sulfur dioxide must be separated, and (3) the operating costs are quite high.

This thesis attempts quantitatively to compare activated carbons produced from waste materials with commercially available activated carbons as an adsorbing media for sulfur dioxide. It should be noted that the use of activated carbon produced from waste materials is only one of a number of possibilities for waste utilization.

Adsorption is the ability of certain solids to concentrate specific substances from solution onto their surfaces. The net result from this phenomenon is a component separation of the gaseous or liquid phase. All solids will adsorb to some degree, the extent of which depends upon the adsorbent in question and the component being adsorbed. Activated carbon is particularly selective toward non-polar molecules such as hydrocarbons, while activated silica and

alumina are highly adsorbent toward water and other polar molecules [17].

By far, the most widely used adsorbent today is activated carbon. It can be made from a variety of materials such as coal, wood, nut shells, dried bones, and fruit pits. These materials are usually dried, crushed, and then heated to high temperatures in an inert atmosphere until most of the volatile components are removed. Activation occurs when steam is passed through the remaining carbon and ash. Occasionally phosphoric or sulfuric acid is used to increase the activation by creating a greater surface area. Typical surface areas for activated carbons used in gas masks are in the order of one million square meters per kilogram.

The three basic industrial uses for activated carbon are decolorization, liquid purification, and gas purification. A major industrial area for which decolorization is used is in refining sugar. Animal bone makes the best adsorbent for this purpose. Liquid purification is used extensively in the purification of chemicals, drugs, dry cleaning liquids, water, and oils of vegetable and animal origin. The best adsorbent carbons for this purpose are made from vegetable matter and sawdust. One of the first applications of gas purification was in the manufacture of gas masks during World War I. This technology quickly spread into the fields of hydrocarbon fractionation and solvent recovery from gas mixtures. Carbons typically used for this purpose

are produced from coal and fruit pits [27].

The characteristics of a good adsorbent for flue gas desulfurization are: a high ignition temperature, good regeneration properties, and ease of handling. Adsorption, however, is only the first step of the desulfurization process. Once sulfur dioxide is attached to the micropore surface, reactions then occur with oxygen and water to produce weak concentrations of sulfuric acid. Since coke is regenerated at high temperatures in an inert atmosphere vaporous sulfur dioxide, sulfur trioxide, carbon dioxide, and water are formed and must be dealt with by additional processing.

To compare quantitatively activated carbon produced from waste materials with commercial activated carbons currently used in sulfur dioxide removal, a packed-bed adsorber was used. Figure 1 depicts a packed-bed adsorber column of fixed geometry and packed with adsorbent particles. The deposition of solute on the adsorbing medium from the feed stream results in a concentration gradient within the column in the direction of flow. This profile is known as the adsorption wave. As soon as any part of the column approaches complete saturation, it becomes practically inert, and this activation is accompanied by a progressive advance of the adsorption wave in the direction of gas flow. Concentration of the flowing fluid at the effluent end of the column is said to trace out a "breakthrough" curve [16].

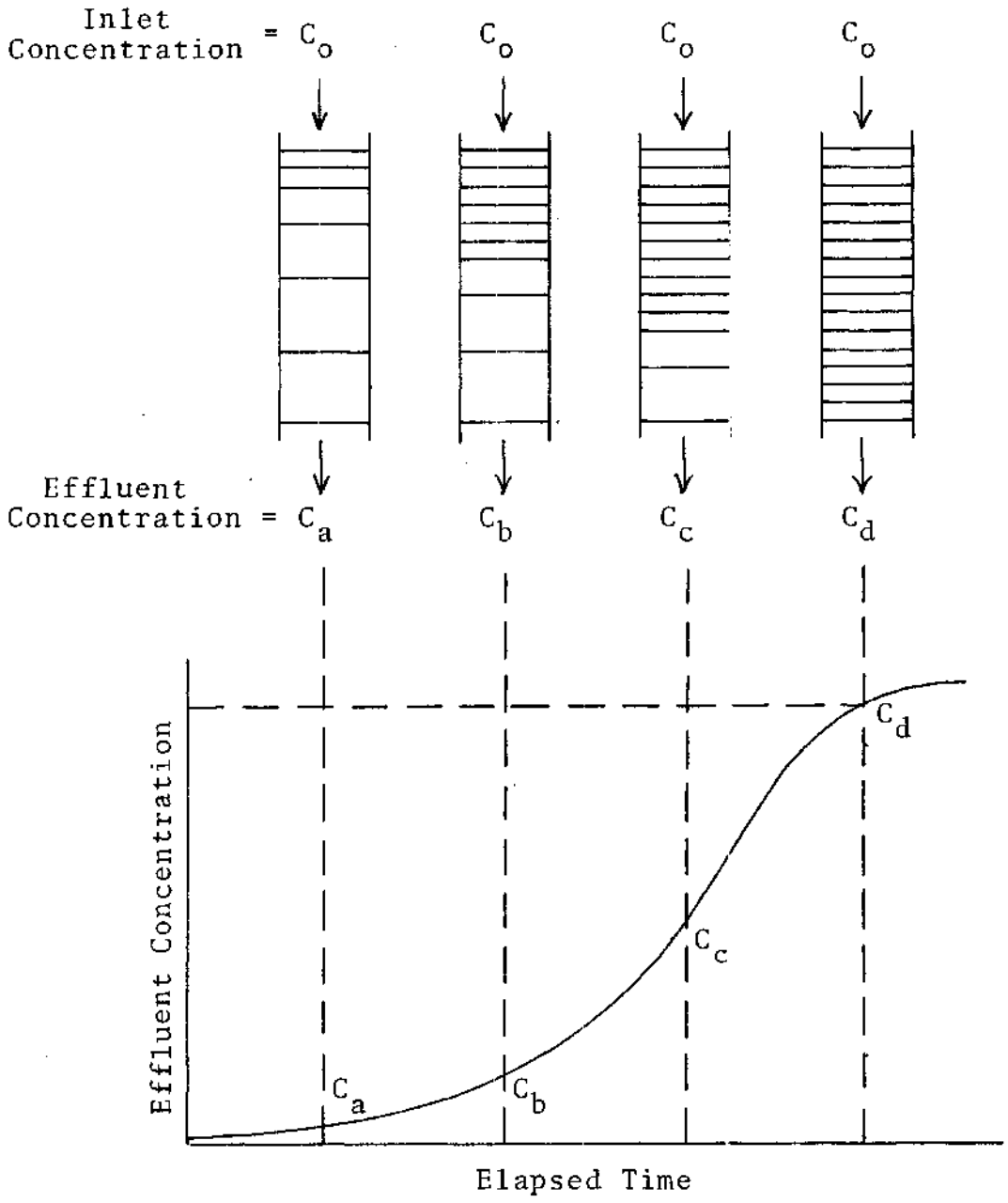

Figure 1. Plot of Effluent Gas Concentration with Elapsed Time

When the effluent concentration reaches the breakpoint, the rate of adsorption decreases drastically; the feed to the column must be discontinued. Regeneration of the adsorbent is then necessary for adsorbate recovery or for adsorbent reuse.

A literature search revealed that adsorption became industrially important during World War I when it was necessary to produce gas masks for use in chemical warfare. Bohart and Adams [5] developed an equation to predict the effluent gas concentration from fixed-bed adsorption as a function of time and bed depth by assuming irreversible adsorption with surface kinetics controlling. Their results, however, did not correlate well with data obtained for chlorine fixed-bed adsorption.

In 1939, Wicke [21] presented his solution for the case of a linear equilibrium curve and a very fast adsorption rate. Only a portion of his experimental data supported his solution. DeVault [11] also assumed that the rate of adsorption was very fast, and extended Wicke's work by assuming that the shape of the breakthrough curve was determined not by longitudinal diffusion, but by the shape of the equilibrium curve. He showed that a favorable equilibrium curve led to a "self-sharpening" breakthrough curve. A curve such as this tends to become steeper with increasing bed depth. Also he found that a linear equilibrium curve results in a constant pattern profile; that is, the

breakthrough curve remains unchanged in shape as it passes through the bed. He showed that unfavorable equilibrium gives rise to what is known as proportionate pattern breakthrough curves. Such curves become flatter or more diffuse with increasing bed depth. Walter [30] later extended this approach to multicomponent adsorption.

Thomas [24,25], who was the first to obtain a solution where internal resistance was controlling, postulated a diffusional rather than a kinetic rate equation for adsorption. He assumed linear equilibrium for this work. On the basis of the film concept, Rosen [22] solved the problem with both internal and external resistance negligible. He reported numerical results for his solution that correlated closely with his experimental results.

Michaels [8] proposed a general technique which has gained wide acceptance as a design method. He defined an "exchange zone" in which the fluid concentration increases from 5% to 95% of its final value and the shape of the breakthrough curve is constant. His procedure requires an experimental breakthrough curve with known exchange zone length and extent of zone saturation. If known, these parameters can be used to size an adsorption column. Camp [6] used a more recent method for adsorption analysis. In his work breakthrough curves at three bed positions were obtained. Using this procedure the concentration profile can be estimated at a given time with respect to bed depth.

With the above background, the following question arises. Do the models accurately represent adsorption? Answering this question has been the goal of many experimenters. It has been customary to assume that the adsorption process being considered may be represented by a given model if the experimental breakthrough curves can be superimposed on the theoretical ones without serious deviation. Such techniques have been applied to ion exchange resins by Dranoff and coworkers [10,13,28], to silica gel by Masamune and Smith [18, 19], and to zeolites by Barrer [2]. Since reasonable curve fits to the theoretical breakthrough curves were obtained by all of the above investigators, the models corresponding to these theoretical curves were assumed to represent the adsorption process being studied. It is expected that at high flowrates, external film diffusion would be rapid and intraparticle diffusion would control the adsorption process. This argument seems plausible in light of Habgood's [14] work in which it was shown that the microscopic openings through which the adsorbate must diffuse are serious hindrances to intraparticle diffusion.

Activated carbon may have surface areas as great as one million square meters per kilogram thus indicating a very large number of micropores. It is therefore expected that the adsorption of sulfur dioxide onto activated carbon would also be limited by intraparticle diffusion. Rosen's model for this type of adsorption process was employed

because theoretical data for wide ranges of experimental conditions are presented. Nitrogen was used as the carrier gas because it would most likely be the major component for gas mixtures involved in a purification of the gases SO_2, CO_2, etc.

CHAPTER II

THEORY

The technique used in this investigation was to introduce the adsorbate concentration into a fixed bed of activated carbon and then measure the effluent adsorbate concentration as a function of time. For all tests, the adsorbate concentration before the step change was zero. Only one adsorbate, sulfur dioxide, was considered. There are at least three types of information necessary to describe the adsorption behavior. These are (1) an overall mass balance, (2) an equilibrium relationship between the adsorbate concentration in the gas phase to that in the adsorbent phase, and (3) an expression for the adsorption kinetics or rate of adsorption [6].

Mass Balance

For fixed bed adsorption an adsorbate mass balance over a differential section of the column is [23]

$$\text{Input} - \text{Output} = \text{Accumulation}. \tag{1}$$

By assuming transverse homogenity, negligible axial diffusion, plug flow, and independence of volumetric flow on axial position, the mass balance becomes*

*Refer to nomenclature, page vii, for definition of terms.

$$v\left(\frac{\partial c}{\partial z}\right)_t + \rho_b\left(\frac{\partial q}{\partial t}\right)_z + m\left(\frac{\partial c}{\partial t}\right)_z = 0 \qquad (2)$$

Upon introducing the following variable changes:

$$\lambda = \rho_b \, z/v \qquad (3)$$

and

$$\theta = t - zm/v \qquad (4)$$

the adsorbate material balance may be written in dimensionless form as

$$\left(\frac{\partial c}{\partial \lambda}\right)_\theta = -\left(\frac{\partial q}{\partial \theta}\right)_\lambda \qquad (5)$$

Equilibrium Considerations

For reversible adsorption three types of equilibrium isotherms exist. These are classed as (a) unfavorable, (b) linear, and (c) favorable isotherms. Examples are shown in Figure 2 [29].

Types (a) and (b) are usually described by a Langmuir or Freundlich relationship. However, most of the available adsorption kinetic models are based on the assumption that a linear isotherm exists and an equilibrium coefficient K_D is defined by the equation:

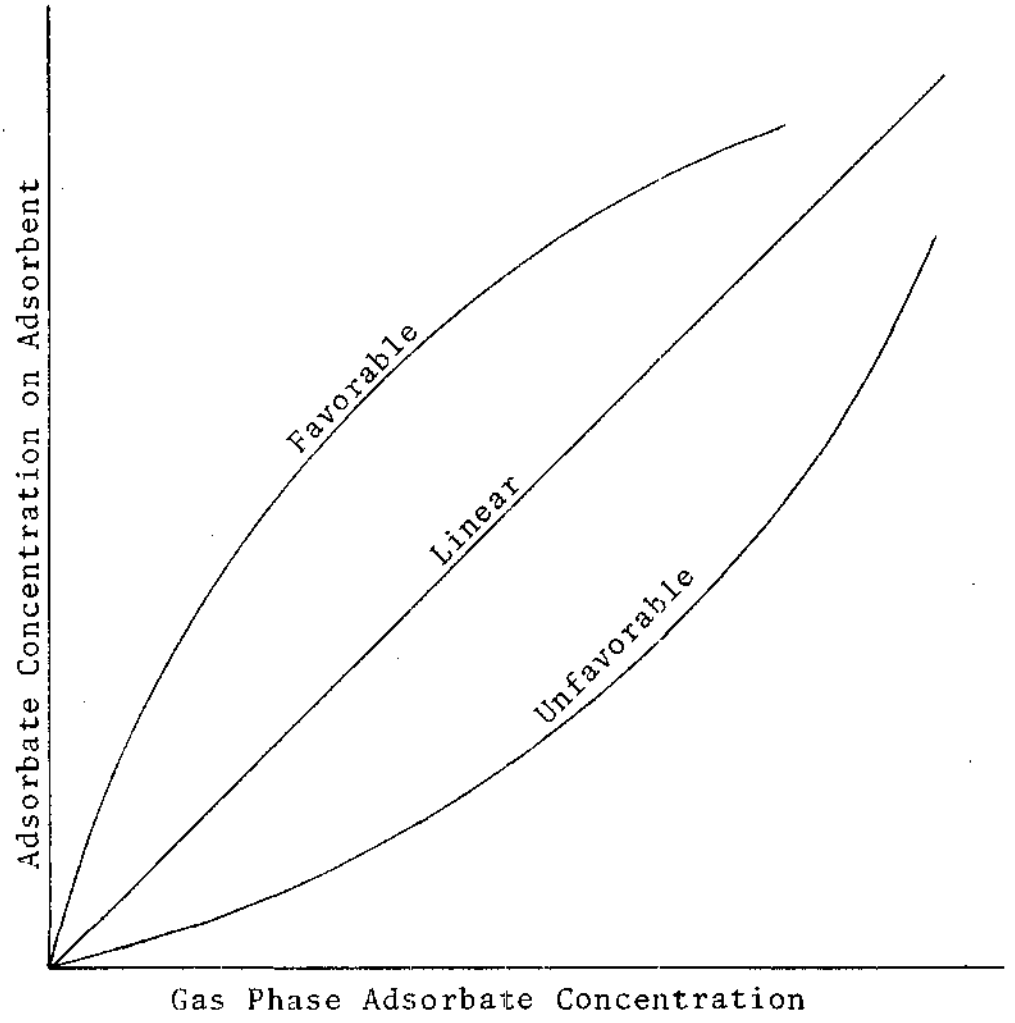

Figure 2. Types of Equilibrium Isotherms

$$K_D = q/c \tag{6}$$

where c is the gas phase adsorbate concentration, and q is the average adsorbate concentration in the bed. Both q and c are functions of time t and distance z. At the end of each test, the adsorbent bed is very near adsorbate saturation, and is approximately at equilibrium with the gas feed concentration C_o. To evaluate K_D, it is first necessary to calculate q from the following equation:

$$q = \frac{\rho_p}{W} \int_o^t (C_o - C)G \, dt \tag{7}$$

K_D may then be found from equation (6).

Kinetics of Adsorption

In adsorption four possible rate limiting steps must be considered. These are (1) external mass transfer, (2) pore diffusion, (3) surface reaction, and (4) internal solid phase diffusion. If these four adsorption steps represent the total resistance to adsorption then the general solution describing the adsorption process must include all four relationships. Simplifications may usually be made, however, when one adsorption rate is much slower than the remaining three. Under these conditions the slower step would be rate limiting. The adsorption kinetics can thus be closely approximated by the kinetics of this single step. The

preceding condition is often the case and this approximation is usually made [7].

Rosen's Solution for Intraparticle and External Diffusivity in Fixed Beds

Due to the large number of micropores found in the activated carbon particle structure, as previously mentioned, intraparticle and external diffusivities are expected to be the most significant rate limiting steps for sulfur dioxide adsorption. It was on these rate limiting steps that Rosen derived his general solution for the effluent concentration in a fixed bed adsorber as a function of time and bed length. He made two primary assumptions: (1) the gas film coefficient and the intraparticle diffusion coefficient are independent of position and concentration over the range of its variation, and (2) the system gives a linear isotherm so that under equilibrium conditions the concentration, q, is proportional to C, the adsorbate concentration in the gas phase of adsorbed material at the surface of the solid.

For adsorption to take place, the adsorbate must first reach the particle surface by diffusing through a static layer of fluid surrounding the particle. From film theory this rate of diffusion is considered to be proportional to the concentration gradient across the film boundary. Rosen assumed that the adsorbent particles were spherical and that the surrounding static layer was uniform. Under these conditions the adsorbate concentration gradient across the film

is $[c - q(b,0,x)/K_D]$ and the rate of mass transfer across the stagnant film is given by

$$\frac{4}{3}\pi b^3 \left(\frac{\partial q}{\partial \theta}\right) = 4\pi b^2 h(c(x,\theta) - q_i(b,x,\theta)/K_D) \tag{8}$$

and

$$\left(\frac{\partial q}{\partial \theta}\right) = \frac{1}{R_f}(c(x,\theta) - q_i(b,x,\theta)/K_D) \tag{9}$$

where

$$R_f = b/3h \tag{10}$$

and

$$h = \text{fluid film coefficient} \tag{11}$$

The average concentration within a particle is given by

$$q(x,\theta) = (3/b^3)\int_0^b q_i(r,x,\theta)r^2 dr \tag{12}$$

Rosen then assumed that diffusion within the particle was limited only by internal phase diffusion and could be defined by the standard spherical diffusion equation

$$\frac{\partial q_i}{\partial \theta} = \frac{D}{r^2} \frac{\partial}{\partial r} \left(r^2 \frac{\partial q_i}{\partial r}\right) \tag{13}$$

By nondimensionalizing the concentration,

$$u(o,\theta) = c(o,\theta)/C_o \tag{14}$$

and using the boundary conditions

$$q_i(r,x,\theta) = 0 \qquad 0 \leq r \leq b,\ x \geq 0,\ \theta = 0 \tag{15}$$

$$u(0,\theta) = 0 \qquad \theta = t \leq 0 \tag{16}$$

$$u(0,\theta) = 1 \qquad \theta = t > 0 \tag{17}$$

he solved for u as a function of surface resistance ν, effective bed length x, and adsorbate contact time y. His solution is

$$u(\nu,x,y) = \frac{1}{2} + \frac{1}{\pi} \psi(\nu,x,y) \tag{18}$$

where

$$\psi(\nu,x,y) = \int_o^\infty e^{-xH_1(\sqrt{\beta},\nu)} \sin[y\beta - xH_2(\sqrt{\beta},\nu)] \frac{d\beta}{\beta} \tag{19}$$

and

$$x = 3DKZ/mvb^2 \text{ (bed length)} \tag{20}$$

$$y = 2D(t - z/v)/b^2 \text{ (contact time)} \tag{21}$$

$$\nu = 3DKR_f/b^2 \text{ (film resistance).} \tag{22}$$

In a later paper Rosen [22] showed that for values of x greater than 0.2 equation 19, could be approximated by

$$u = \frac{1}{2} + \frac{1}{2} \operatorname{erf} \left(\frac{3y/2x-1}{2\sqrt{\frac{1+5\nu}{5x}}}\right) \tag{23}$$

with an error of no greater than 0.002. For $\nu = 0$ the solution is

$$(u)_{\nu=o} = \frac{1}{2} + \frac{1}{2} \operatorname{erf} \left(\frac{3y/2x-1}{2/\sqrt{5x}}\right) \tag{24}$$

and for sufficiently large values of X the solution is

$$u = \frac{1}{2} + \frac{1}{2} \operatorname{erf} \left(\frac{3y/2x-1}{2\sqrt{\nu/x}}\right) \tag{25}$$

CHAPTER III

APPARATUS AND PROCEDURE

For this investigation activated carbon was made from peanut hulls and waste rubber via high temperature carbonization and steam activation. Two commercially available activated carbon products were also tested to provide assistance to the investigator's evaluation. Activated carbons, rated for both air and water purification processes, from the two companies Westvaco and Barnebey Cheney were used for this purpose. All four carbon samples were crushed, sieved to a particle size of between #30 and #45 mesh, and stored in air tight containers.

Preparation of Rubber and Peanut Hull Carbons

The process followed to produce the activated carbon for this investigation was relatively simple. Carbon source material was carbonized at 800°C for 30 minutes in a fourteen inch section of standard two inch pipe fitted with threaded end caps. Activation occurred when steam was injected at a rate of one gram steam per gram of carbon per hour for 30 minutes into the chamber containing the sample which was heated to 800°C. After the activated sample was cooled to room temperature in a nitrogen gas atmosphere, it was promptly removed from the reaction chamber, sieved for particle size

separation, and stored in closed containers in a nitrogen atmosphere. Particle density and bed porosity were determined by water volume displacement using previously weighed samples.

Infrared Analyzer Calibration

A Beckman model 215A infrared analyzer was used to measure the sulfur dioxide concentration and the result was recorded on a Hitachi strip chart recorder. Using the concentration/deflection calibration curves, shown in Figures 32, 33, and 34, experimentally recorded results were corrected for non-linear instrumentation response. This instrument was calibrated for sulfur dioxide in the concentration range from 951 ppm to 11,278 ppm.

For concentration levels of 951 ppm and less, calibration was performed with calibrated gas samples which had been mixed in a 1000 cm^3 stainless steel cylinder fitted with valves at each end. To prepare the sample, the stainless steel cylinder was first purged with pure nitrogen and all valves were closed. A premeasured volume of sulfur dioxide at known temperature and pressure was injected into the sample cylinder through a serum bottle stopper. The cylinder was then filled with nitrogen to a desired pressure. Pressurization with nitrogen was performed at a very slow rate to prevent an increase in sample temperature. Using the known temperature, pressure, and volume, the sample gas concentration

was then calculated. The Beckman infrared analyzer was first adjusted through the strip chart recorder for zero deflection at 0% SO_2 and 100% deflection at 1000 ppm SO_2 in nitrogen. Deflection was then plotted for sample gas concentrations between the upper and lower limit at increments of 100 ppm SO_2 in nitrogen.

For concentrations greater than 951 ppm a different procedure for instrument calibration was used. Here, an initial flow rate of 100% SO_2 was measured at known temperature and pressure with a soap bubble flow meter. Once this flow rate was determined, nitrogen was introduced into the gas stream until a desired flow rate was measured. Using the known temperature, pressure, volume flow rates, and the compressibility factors for the individual gas components, the sample gas concentration was determined. The Beckman infrared analyzer was adjusted for 100% deflection at a desired concentration and a deflection-concentration curve was made for intermediate concentrations.

Apparatus for Adsorption Determination

A schematic diagram of the equipment is shown on page 20 in Figure 3. The nitrogen and sulfur dioxide cylinders were each fitted with a regulator valve for line pressure control, a check valve to prevent contamination, and a needle valve for flow rate control. For changes in gas flow rate or SO_2 concentration only the needle valves were adjusted.

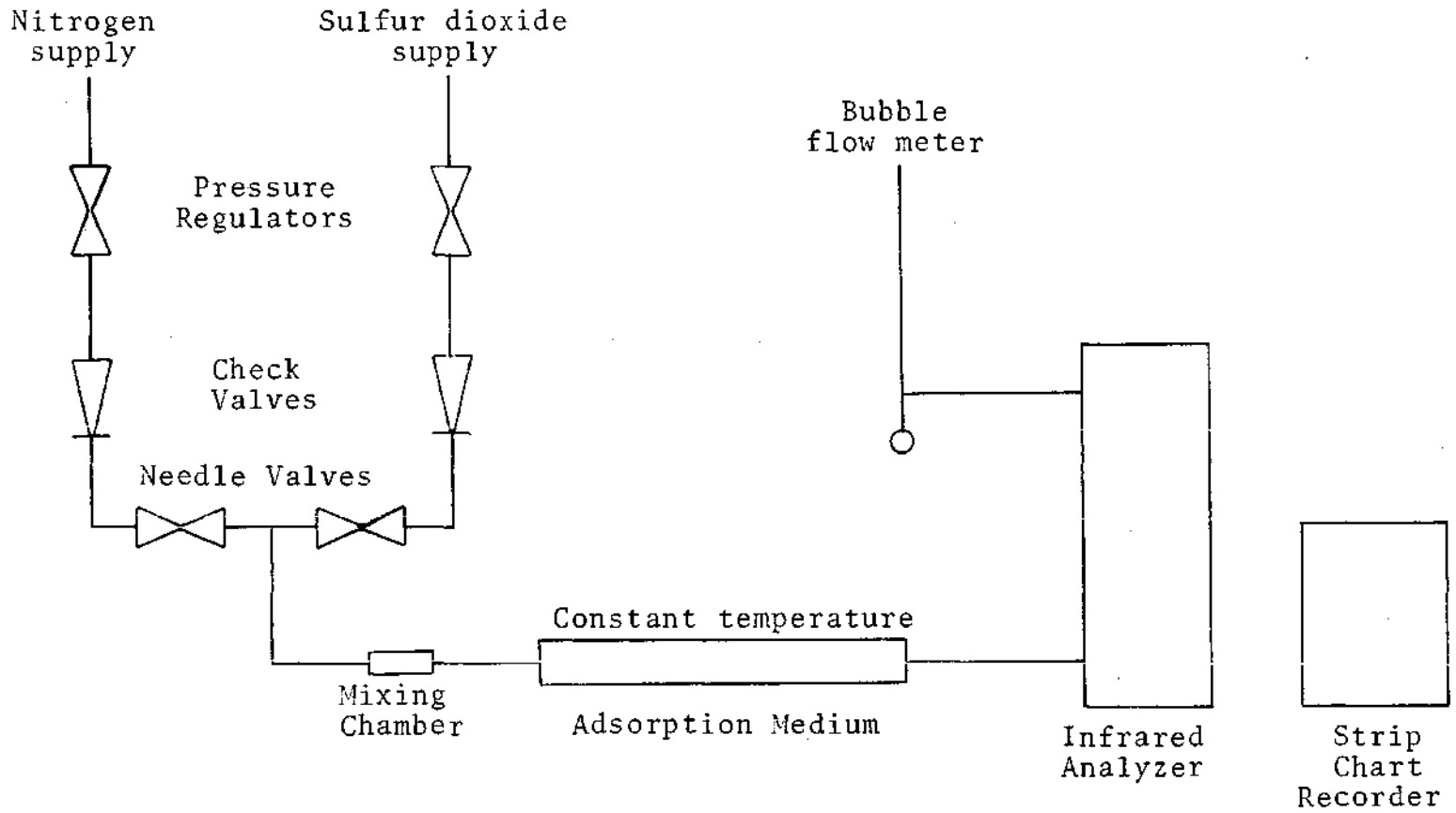

Figure 3. Schematic Diagram of the Apparatus Used for Adsorption Determinations

These valves were connected with 1/4 inch 304 stainless steel tubing. The pure component gases were combined in a mixing 'T' and passed through a column of packed glass beads for further mixing before entering the tube containing the adsorbent. After passing through the adsorbent, the effluent gas was continuously monitored for sulfur dioxide concentration with the infrared analyzer. The flow rate was periodically checked during the run with a bubble flow meter. A by-pass line was installed around the adsorbent tube so that the inlet gas concentration could be checked.

CHAPTER IV

RESULTS

Tables 1, 2, 3, and 4 present the numerical results from this investigation. The tables are organized into three categories based upon the inlet concentration of sulfur dioxide. Within each concentration category, a comparison was made of the intraparticle diffusivities, D, for each activated carbon. Rosen's generalized solution variable, X, was used to calculate intraparticle diffusivities, and the film resistance, R_f, was determined by using equation 25. Activated charcoal from Barnebey Cheney gave breakthrough curves that could only be fitted with Rosen's [22] tabulated values. Changes in gas flow rate or temperature were not studied in this report even though test #1 was made at a flow rate twenty-five percent greater than flow rates used for the remaining tests.

Equilibrium curves relating the sulfur dioxide concentration of the gas phase to that of the solid phase are shown in Figures 4, 5, 6, and 7. Figures 8 through 19 show the experimental breakthrough curves and theoretical curves fits for all adsorption tests. Figures 20 through 31 are desorption plots which were measured after each adsorption test.

Table 1. Test Conditions and Results for Adsorption Experiments Using Carbon from Peanut Hulls

Test	#1	#5	#9
C_o (ppm)	951	5005	11278
C_o (gm SO_2/cm^3)	2.468×10^{-6}	1.285×10^{-5}	2.919×10^{-5}
T (°R)	530.6	532.0	532.0
p (mm Hg)	745	739	745
F (cm^3/min)	413.79	289.85	285.71
G (cm^3/min)	375.86	260.48	258.84
W (gm)	6.9687	6.0363	6.5201
L (cm)	14.7	13.4	13.3
ρ_p (gm/cm^3)	1.3949	1.3949	1.3949
ρ_b (gm/cm^3)	0.2933	0.2730	0.2971
ε	0.7897	0.8043	0.7870
m	3.7560	4.1095	3.6950
$\tau - \int \frac{C}{C_o} d\tau$ (min)	71.59	125.59	72.73
b (cm)	0.0237	0.0237	0.0237
$\vec{v}$ (cm/sec)	4.81	3.27	3.32
q (gm/cm^3)	6.83×10^{-3}	9.71×10^{-2}	1.18×10^{-1}
X	894.79	179.4	705.5
D (cm^2/sec)	7.45×10^{-5}	4.46×10^{-6}	3.08×10^{-5}
K_D	2767	7560	4027

Table 2. Test Conditions and Results for Adsorption Experiments Using Carbon from Waste Rubber

Test	#2	#6	#10
C_o (ppm)	951	5005	11278
C_o (gm SO_2/cm^3)	2.429×10^{-6}	1.28×10^{-5}	2.876×10^{-5}
T (°R)	538	537	539
p (mm Hg)	743.3	743.2	743.2
F (cm^3/min)	408.16	297.03	300.00
G (cm^3/min)	364.668	265.94	267.536
W (gm)	11.7870	7.7383	8.8194
L (cm)	8.8194	14.0	16.1
ρ_p (gm/cm^3)	1.5268	1.5268	1.5268
ρ_b (gm/cm^3)	0.3320	0.3350	0.3320
ε	0.7826	0.7806	0.7826
m	3.5988	3.5576	3.5988
$\tau - \int \frac{C}{C_o} d\tau$ (min)	9.40	16.41	52.55
b (cm)	0.02372	0.02372	0.02372
$\vec{v}$ (cm/sec)	4.71	3.44	3.45
q (gm/cm^3)	6.03×10^{-3}	1.10×10^{-2}	1.25×10^{-2}
X	66.4	34.1	168.5
D (cm^2/sec)	9.64×10^{-6}	6.49×10^{-6}	5.60×10^{-5}
K_D	2482	861	435

Table 3. Test Conditions and Results for Adsorption Experiments Using Carbon from Barnebey Cheney

Test	#3	#7	#11
C_o (ppm)	951	5005	11278
C_o (gm SO_2/cm^3)	2.46×10^{-6}	1.283×10^{-5}	2.865×10^{-5}
T (°R)	532	535	540
p (mm Hg)	745	744	742.0
F (cm^3/min)	289.50	300.00	285.71
G (cm^3/min)	262.273	269.90	254.860
W (gm)	32.1889	19.6695	31.3600
L (cm)	24.7	13.4	22.5
ρ_p (gm/cm^3)	1.6444	1.6444	1.6444
ρ_b (gm/cm^3)	0.7898	0.8896	0.8447
ε	0.5197	0.4590	0.4863
m	1.0820	0.8485	0.9467
$\tau - \int \frac{C}{C_o} d\tau$ (min)	14.05	14.61	100.38
b (cm)	0.02372	0.02372	0.02372
$\vec{v}$ (cm/sec)	5.10	5.94	5.29
q (gm/cm^3)	3.31×10^{-3}	4.23×10^{-3}	5.39×10^{-3}
X	0.2	1.0	2.0
D (cm^2/sec)	6.23×10^{-9}	2.14×10^{-7}	4.45×10^{-7}
K_D	1345	330	188

Table 4. Test Conditions and Results for Adsorption Experiments Using Carbon from Westvaco

Test	#4	#8	#12
C_o (ppm)	951	5005	11278
C_o (gm SO_2/cm^3)	2.457×10^{-6}	1.284×10^{-5}	2.909×10^{-5}
T (°R)	533	537	534
p (mm Hg)	744.8	744.5	745.1
F (cm^3/min)	285.71	288.46	284.36
G (cm^3/min)	258.284	258.724	256.685
W (gm)	14.6191	17.7143	13.3801
L (cm)	14.3	17.7	13.4
ρ_p (gm/cm^3)	1.6511	1.6511	1.6511
ρ_b (gm/cm^3)	0.6196	0.6066	0.6052
ε	0.6247	0.6326	0.6334
m	1.6648	1.7219	1.7282
$\tau - \int \frac{C}{C_o} d\tau$. (min)	77.27	143.71	159.85
b (cm)	0.02372	0.02372	0.02372
$\vec{v}$ (cm/sec)	4.18	4.13	4.09
q (gm/cm^3)	1.14×10^{-2}	4.45×10^{-2}	7.12×10^{-2}
X	53.8	111.3	80.0
D (cm^2/sec)	1.05×10^{-6}	2.42×10^{-6}	3.23×10^{-6}
K_D	4663	3466	2448

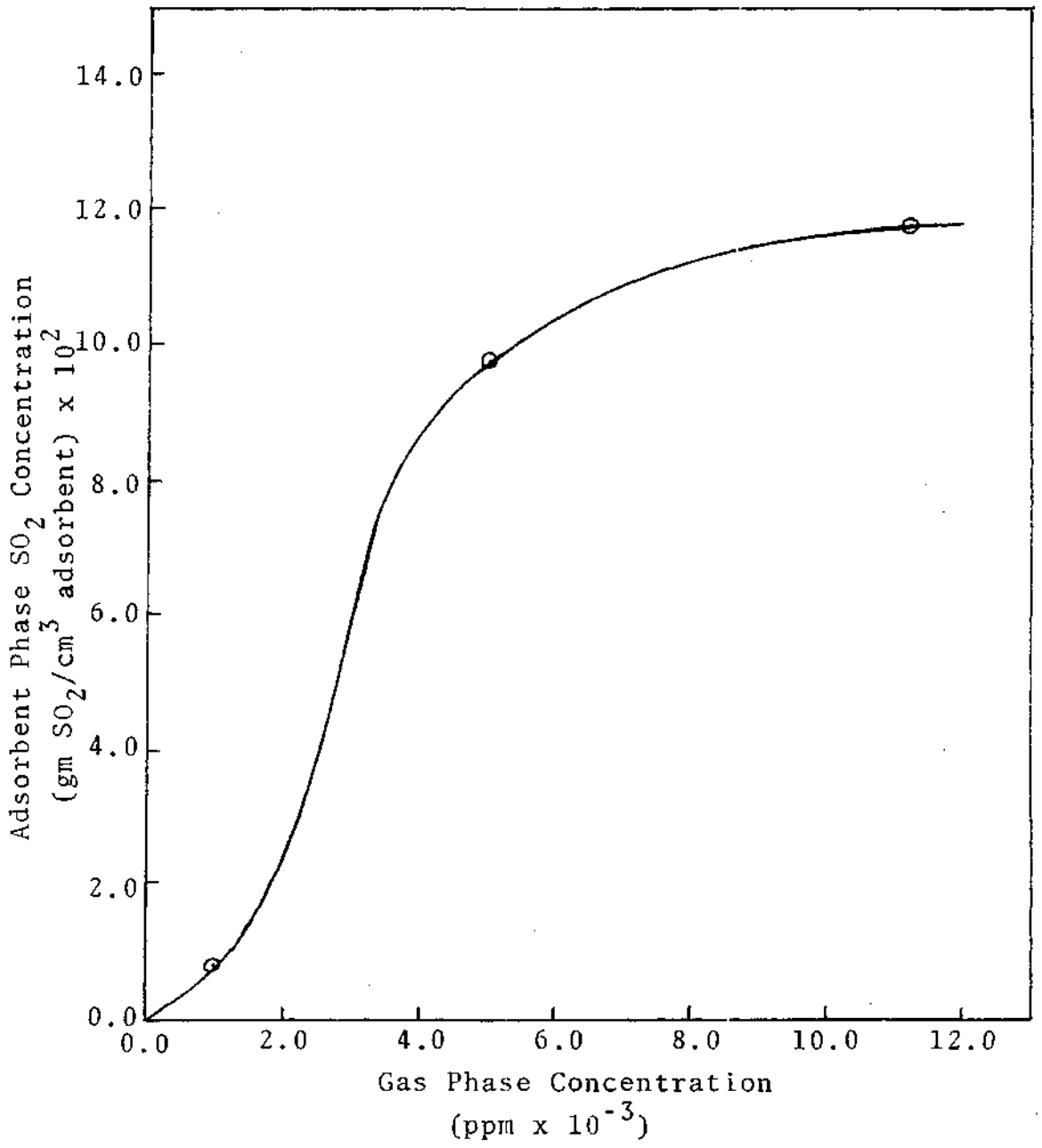

Figure 4. Isotherm for Activated Carbon Produced from Peanut Hulls

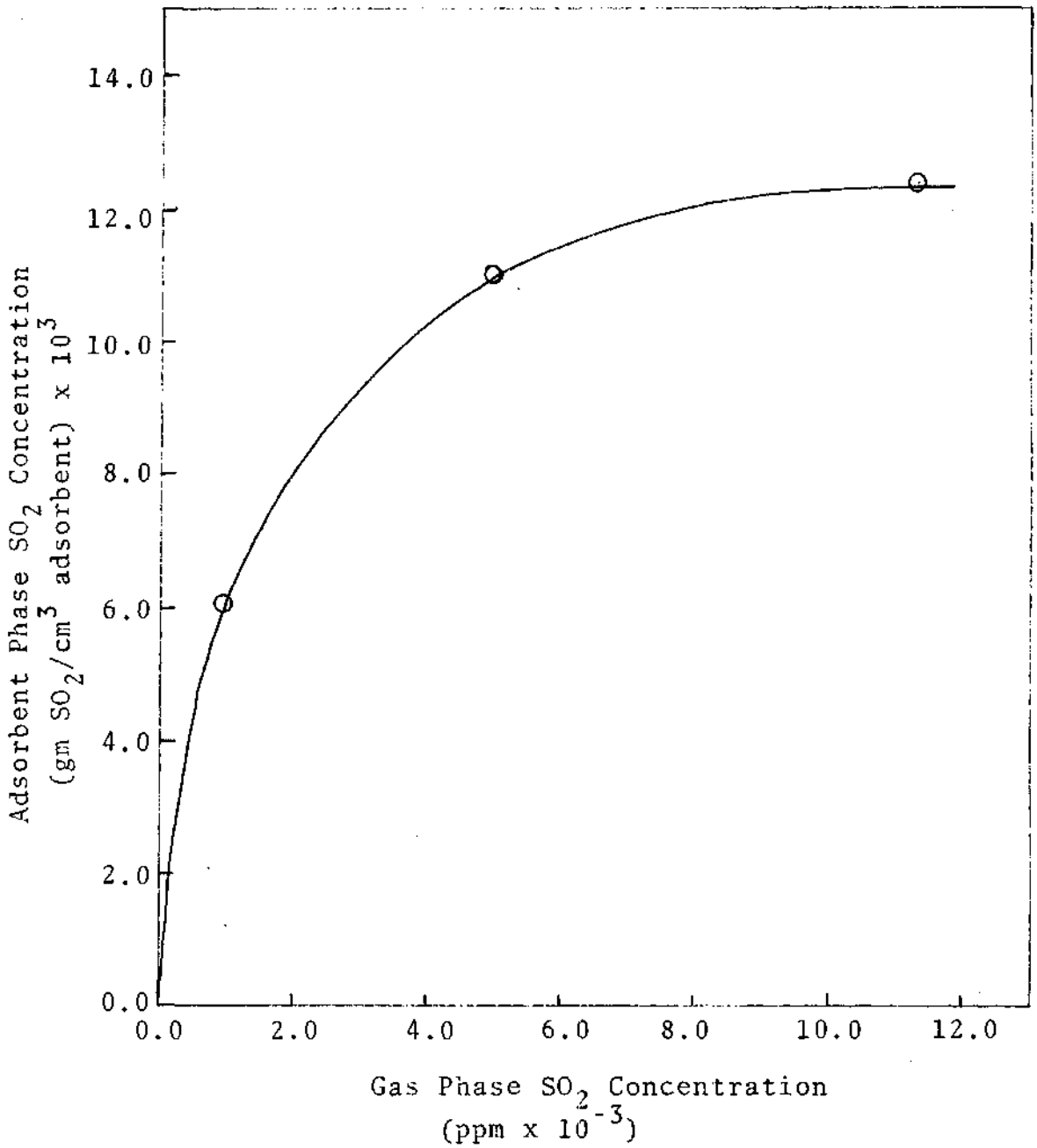

Figure 5. Isotherm for Activated Carbon Produced from Waste Rubber

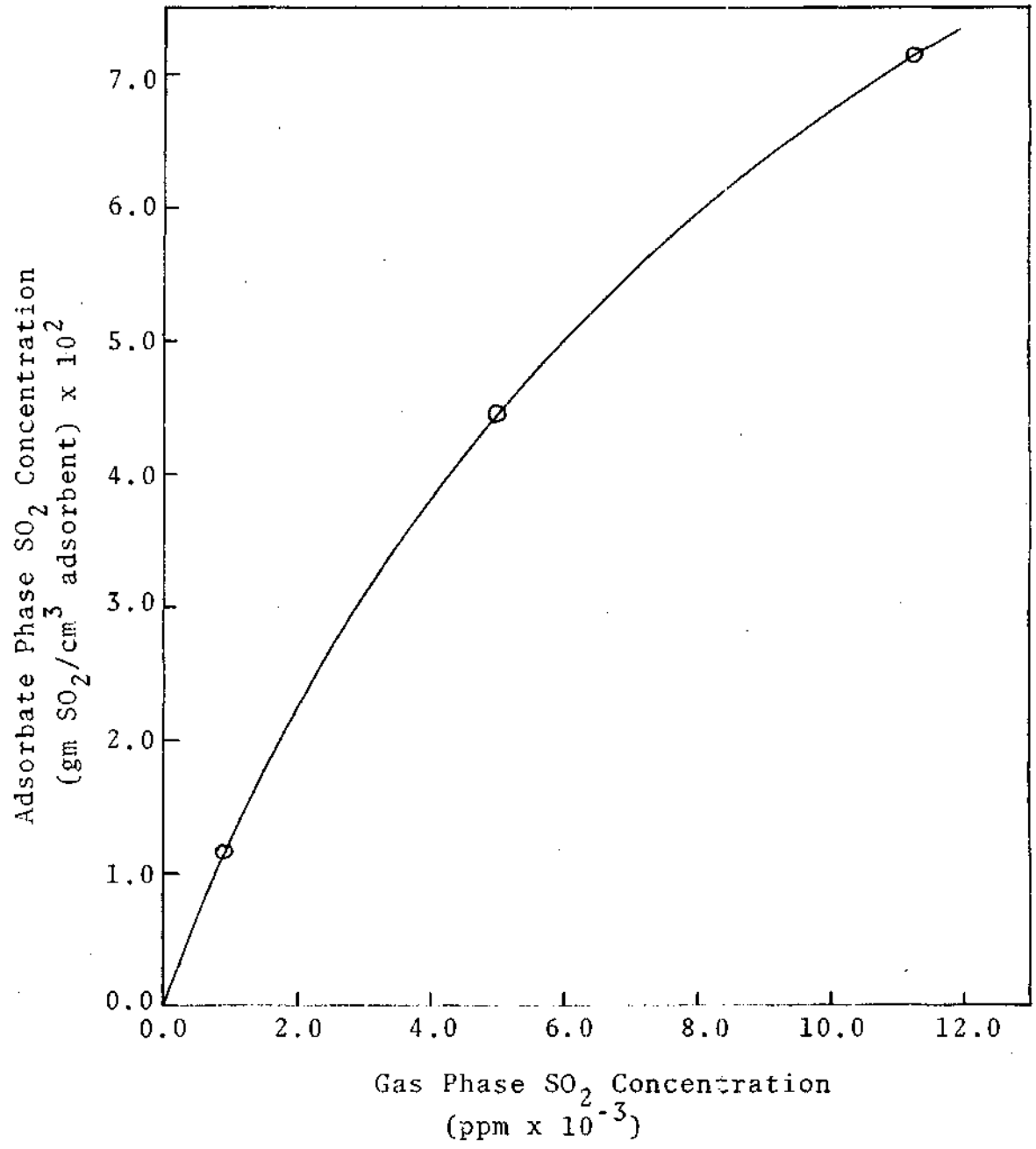

Figure 6. Isotherm for Activated Carbon Produced by Westvaco

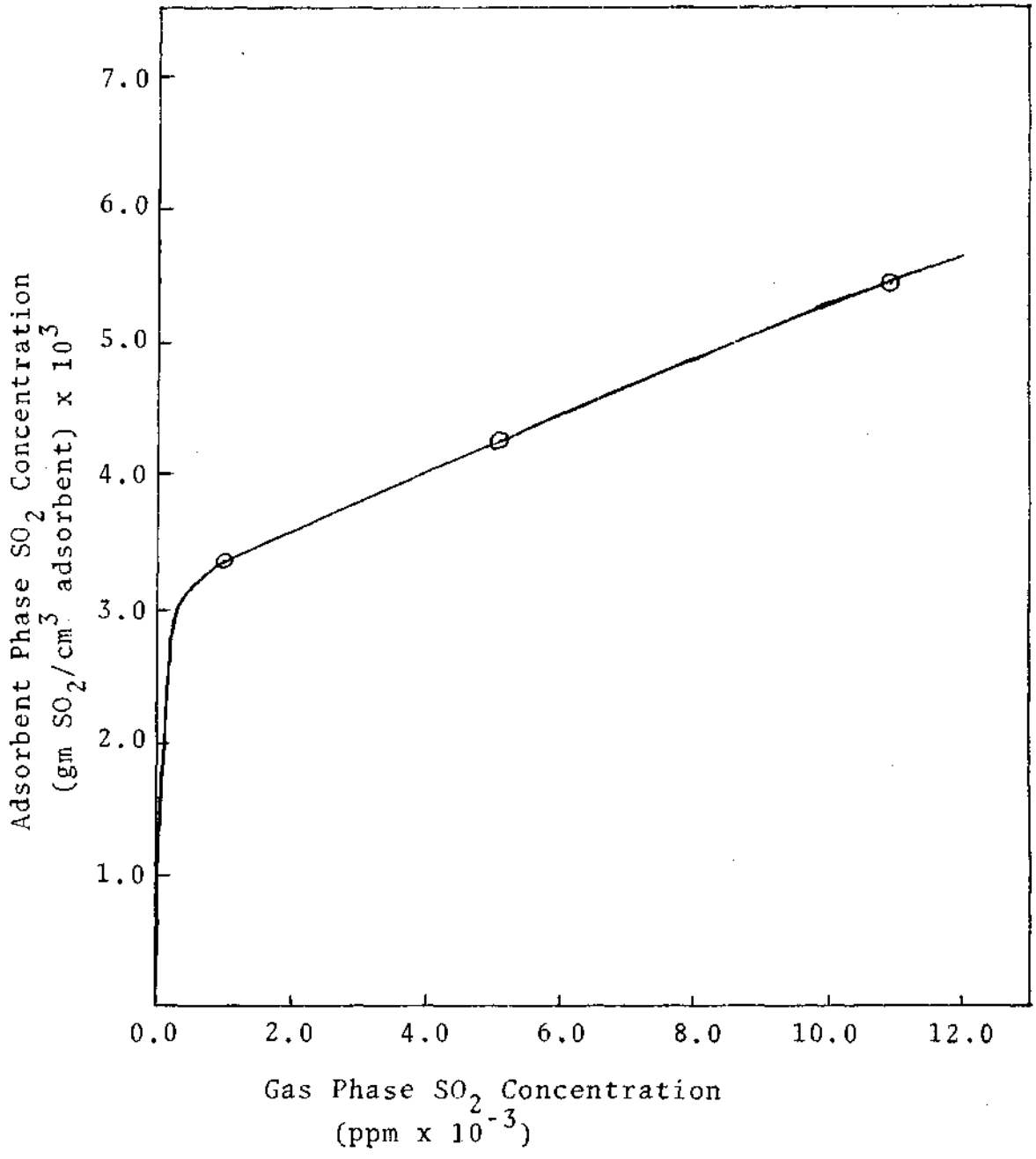

Figure 7. Isotherm for Activated Carbon Obtained by Barnebey Cheney

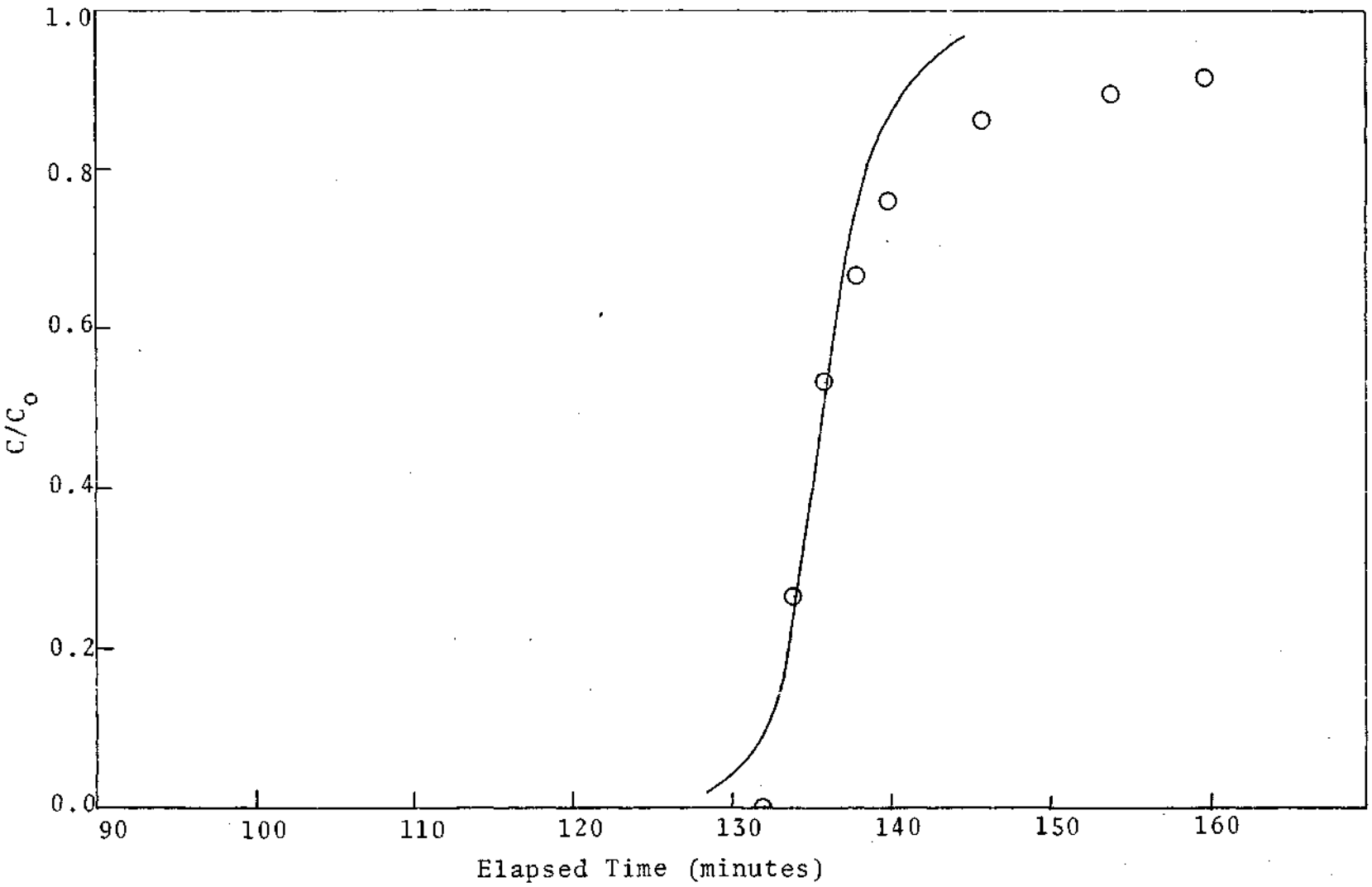

Figure 8. Breakthrough Curve for Test #1

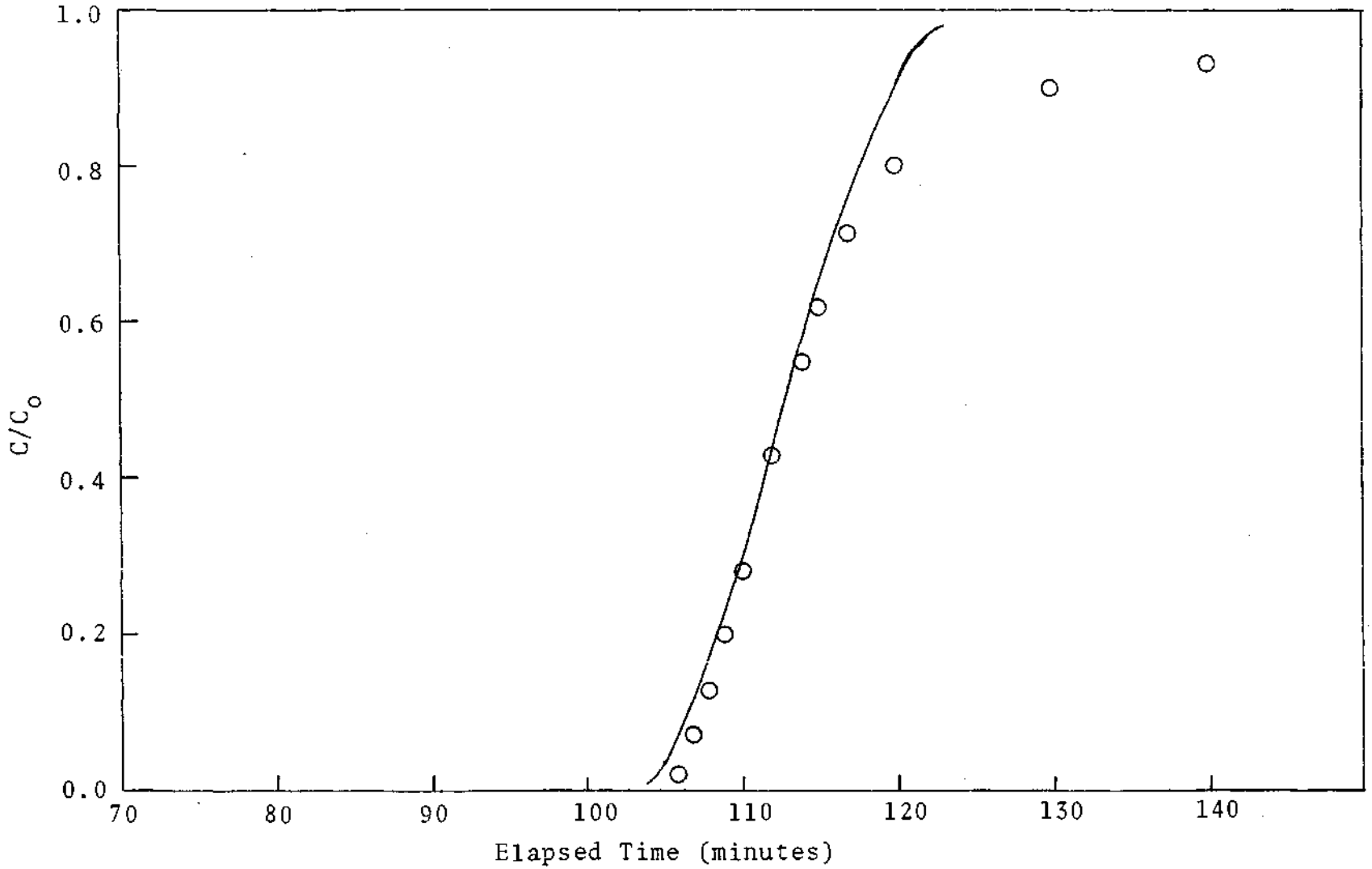

Figure 9. Breakthrough Curve for Test #5

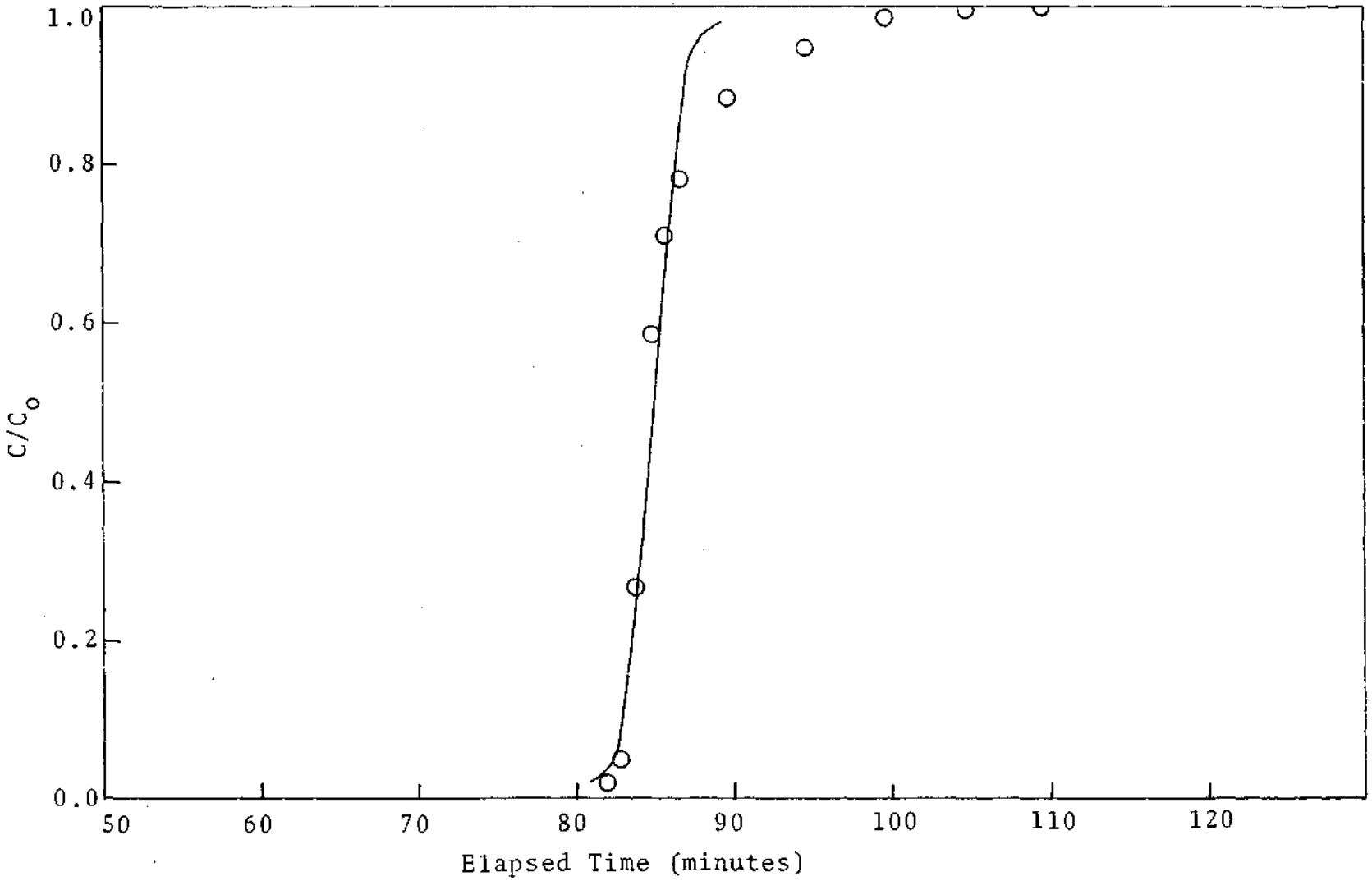

Figure 10. Breakthrough Curve for Test #9

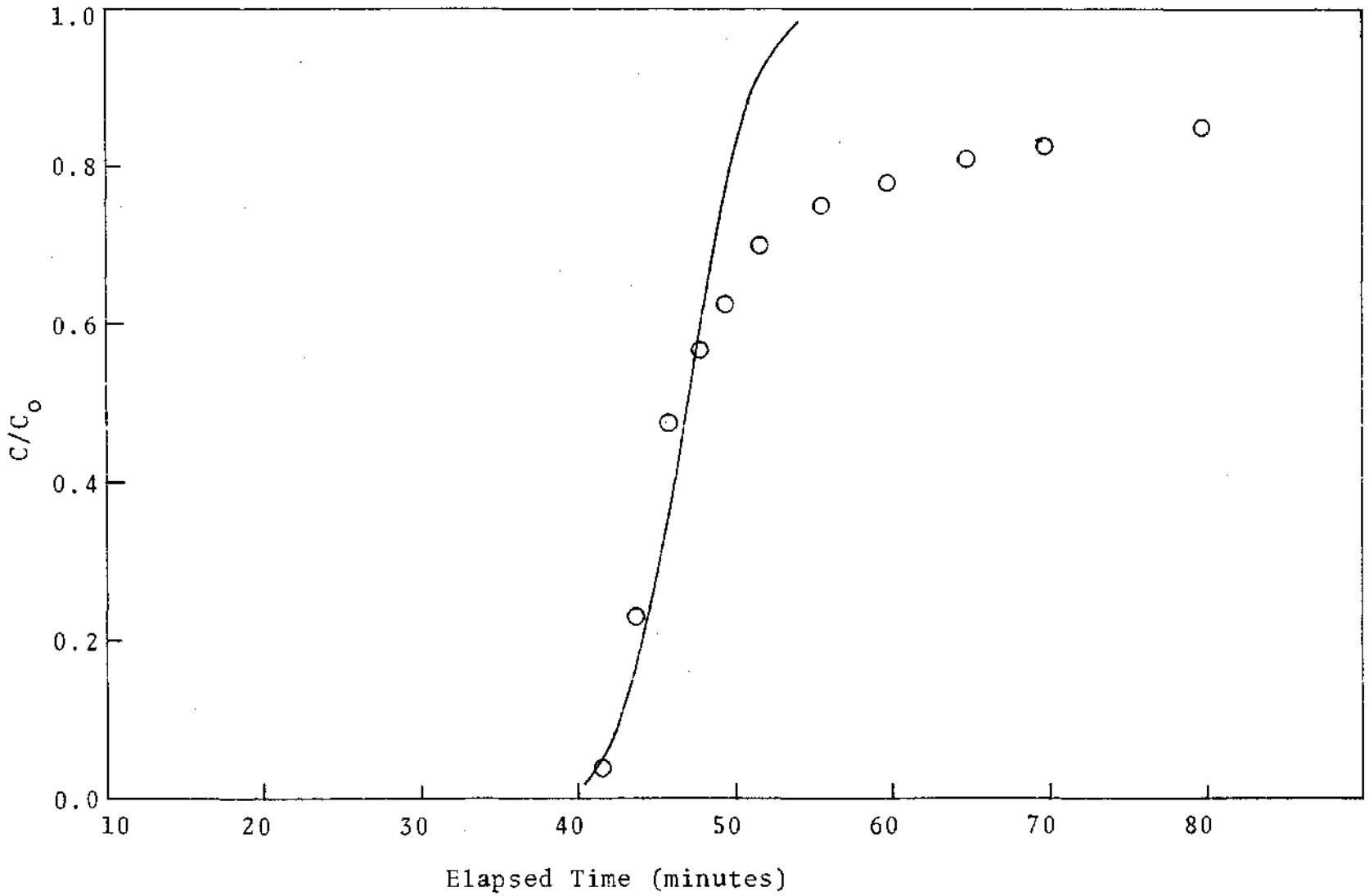

Figure 11. Breakthrough Curve for Test #2

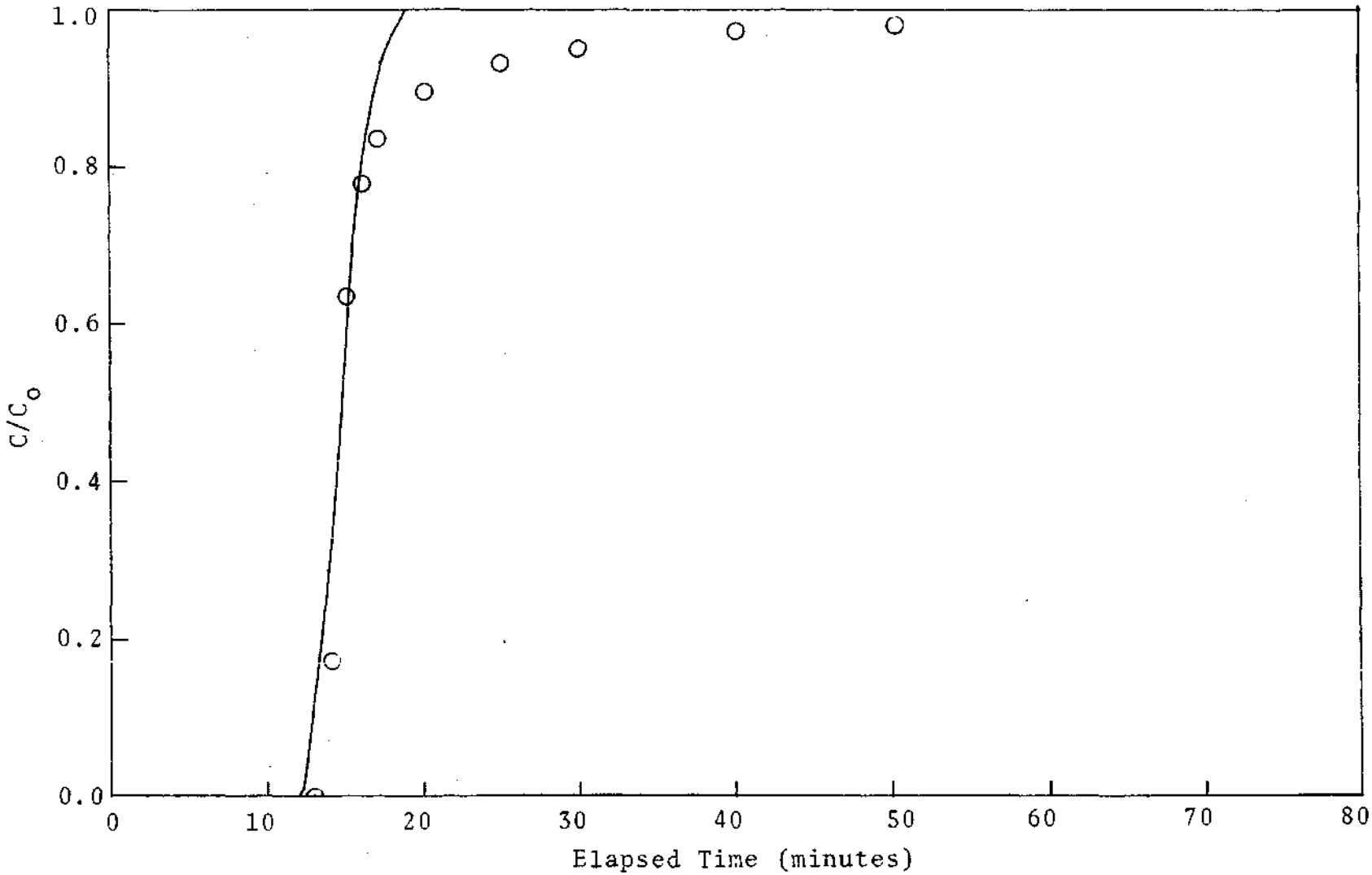

Figure 12. Breakthrough Curve for Test #6

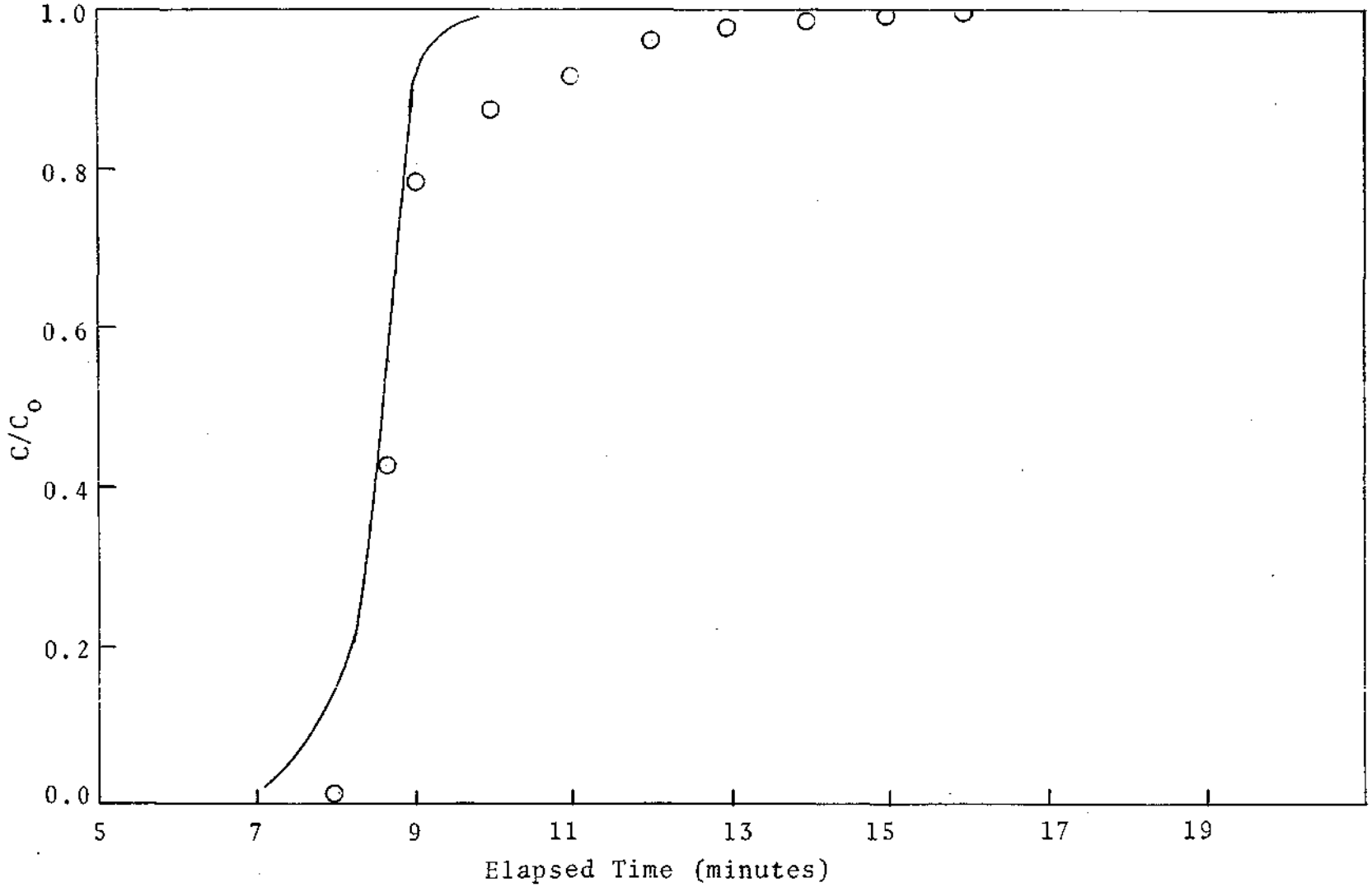

Figure 13. Breakthrough Curve for Test #10

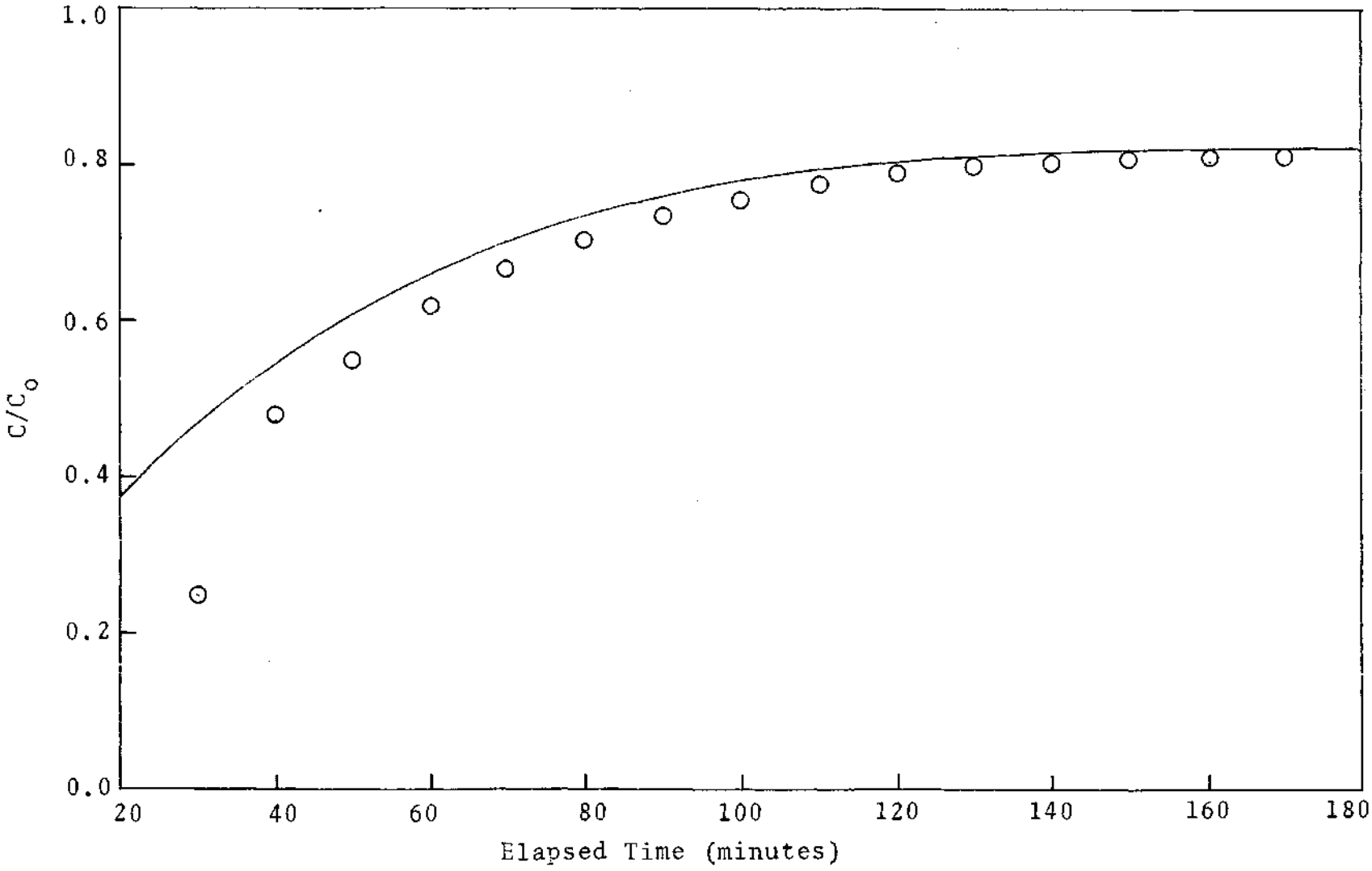

Figure 14. Breakthrough Curve for Test #3

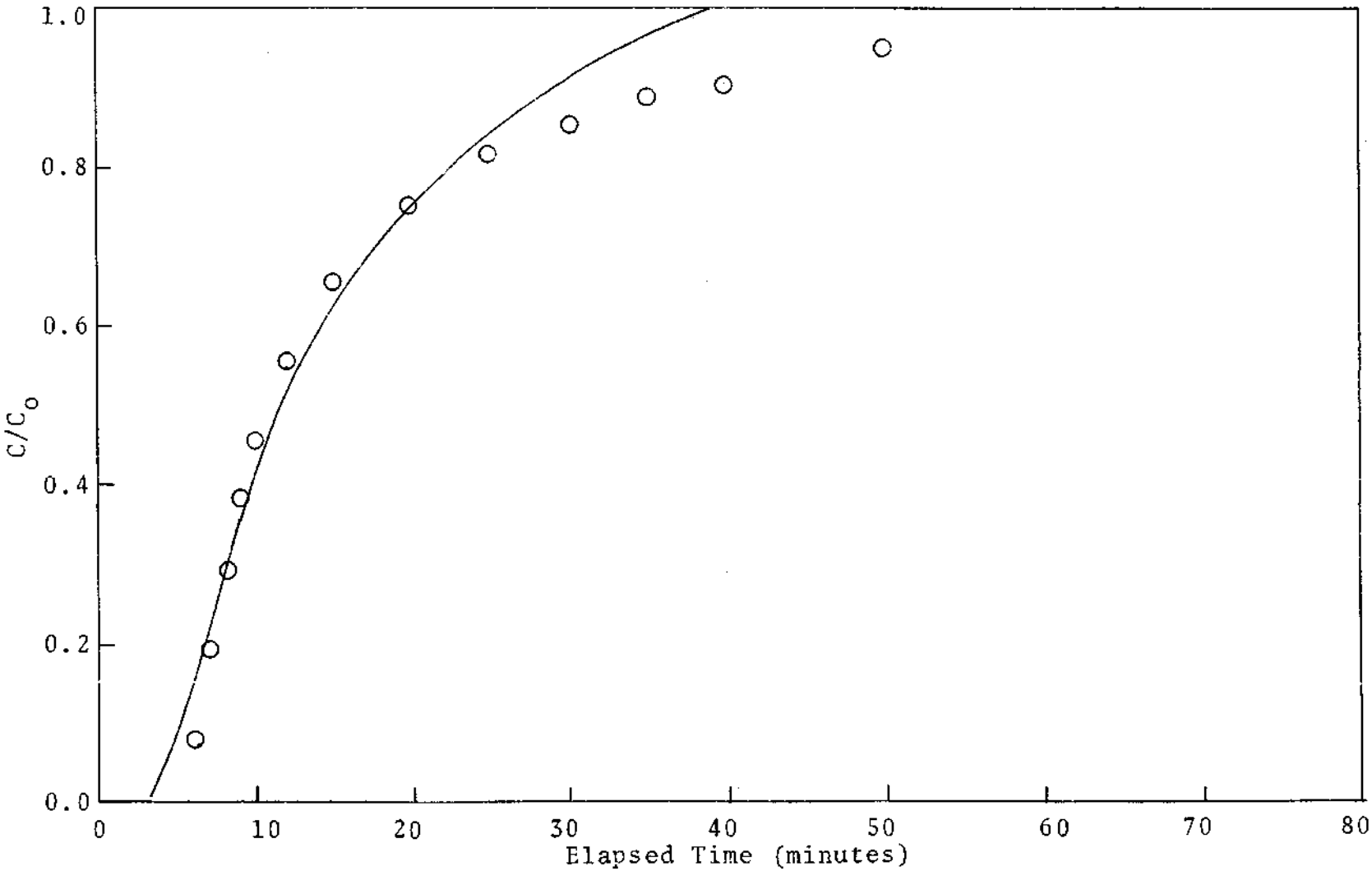

Figure 15. Breakthrough Curve for Test #7

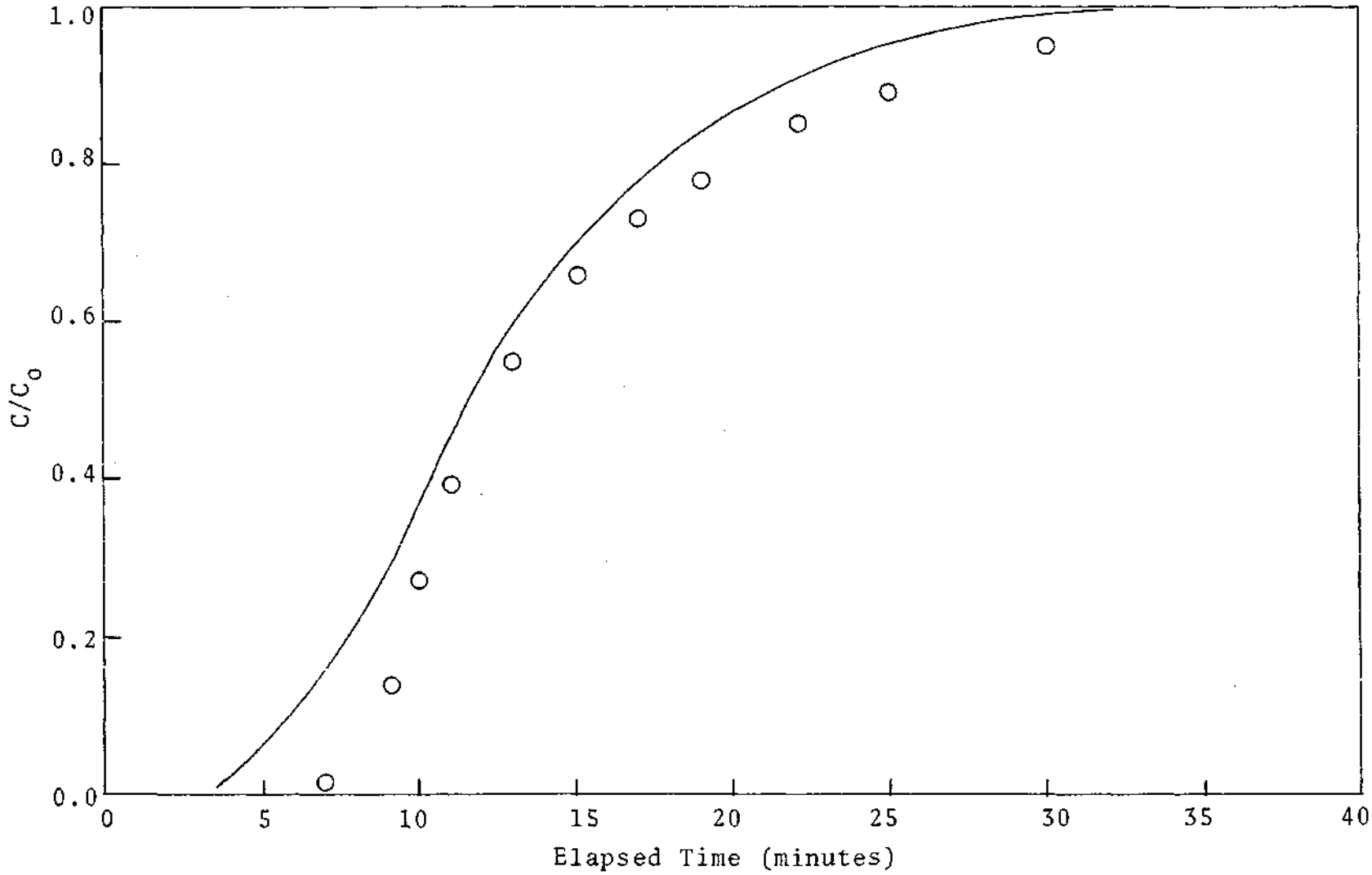

Figure 16. Breakthrough Curve for Test #11

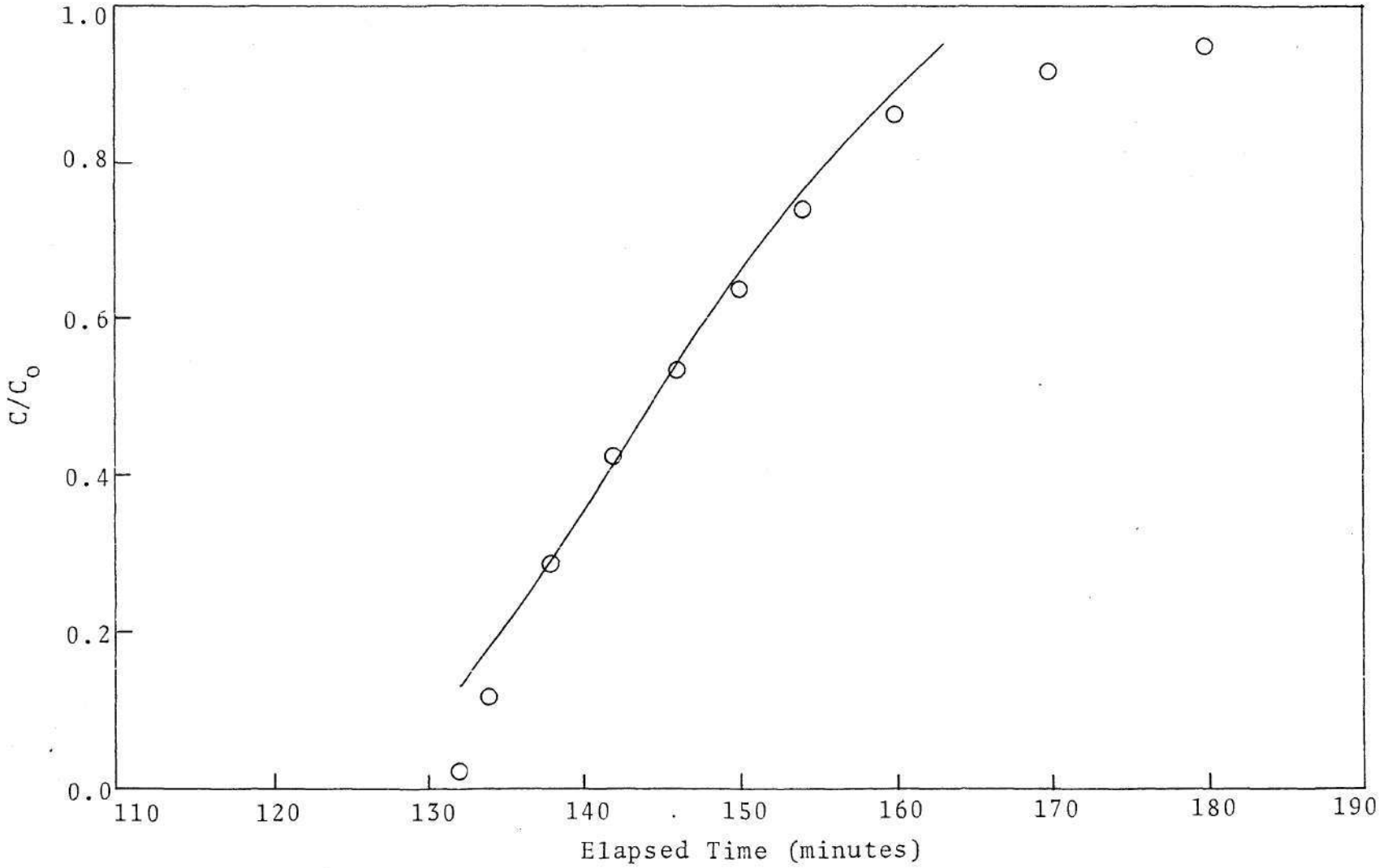

Figure 17. Breakthrough Curve for Test #4

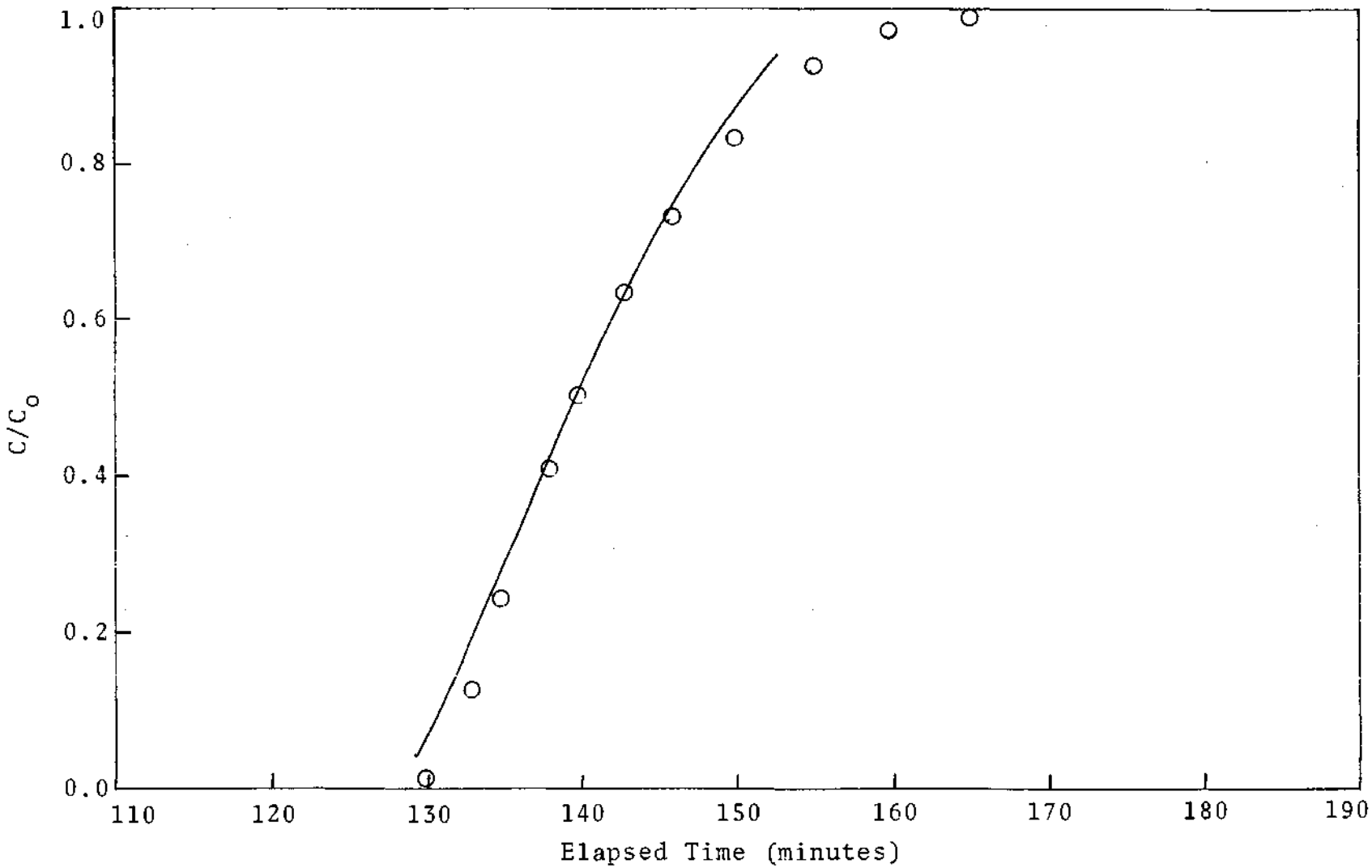

Figure 18. Breakthrough Curve for Test #8

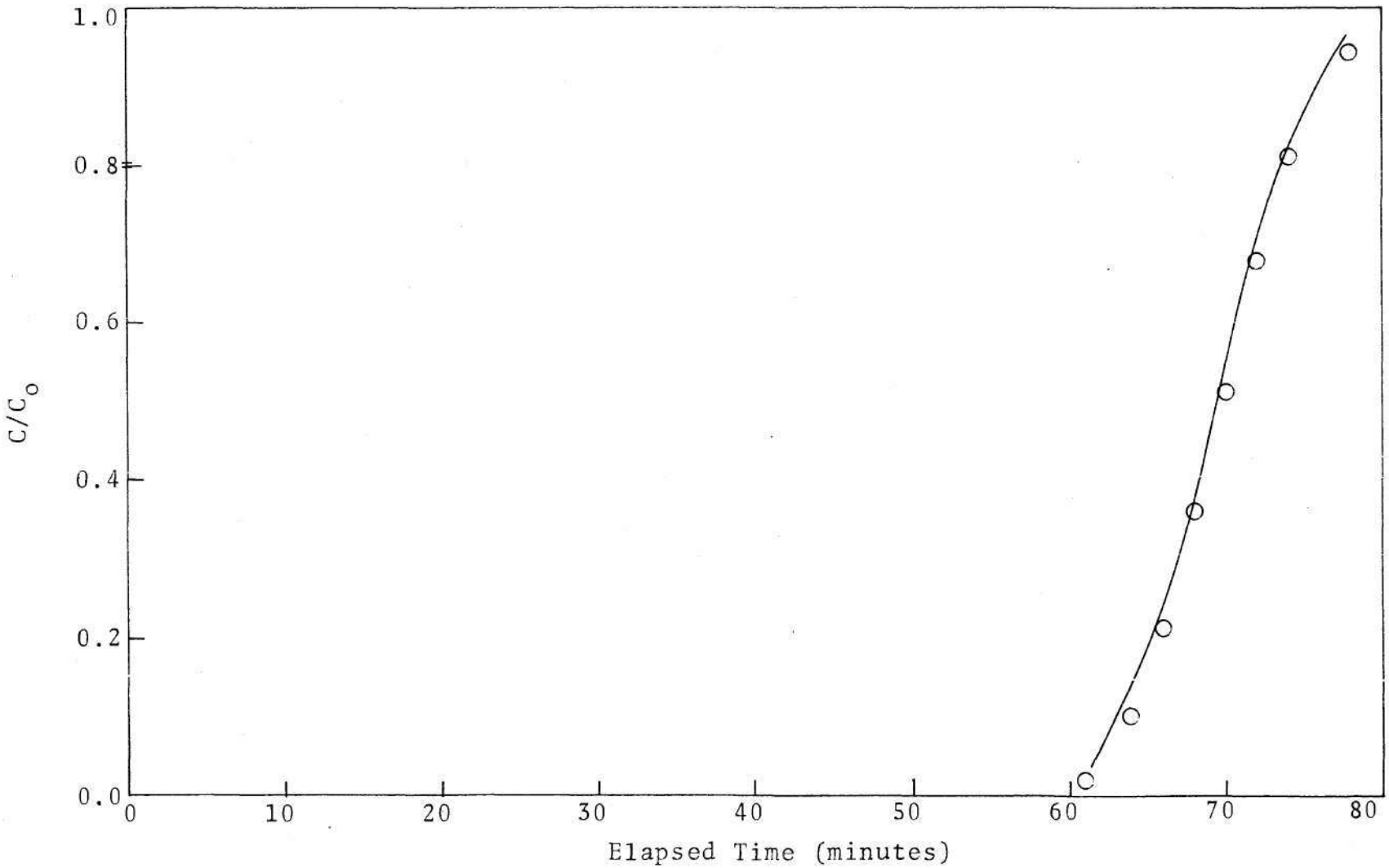

Figure 19. Breakthrough Curve for Test #12

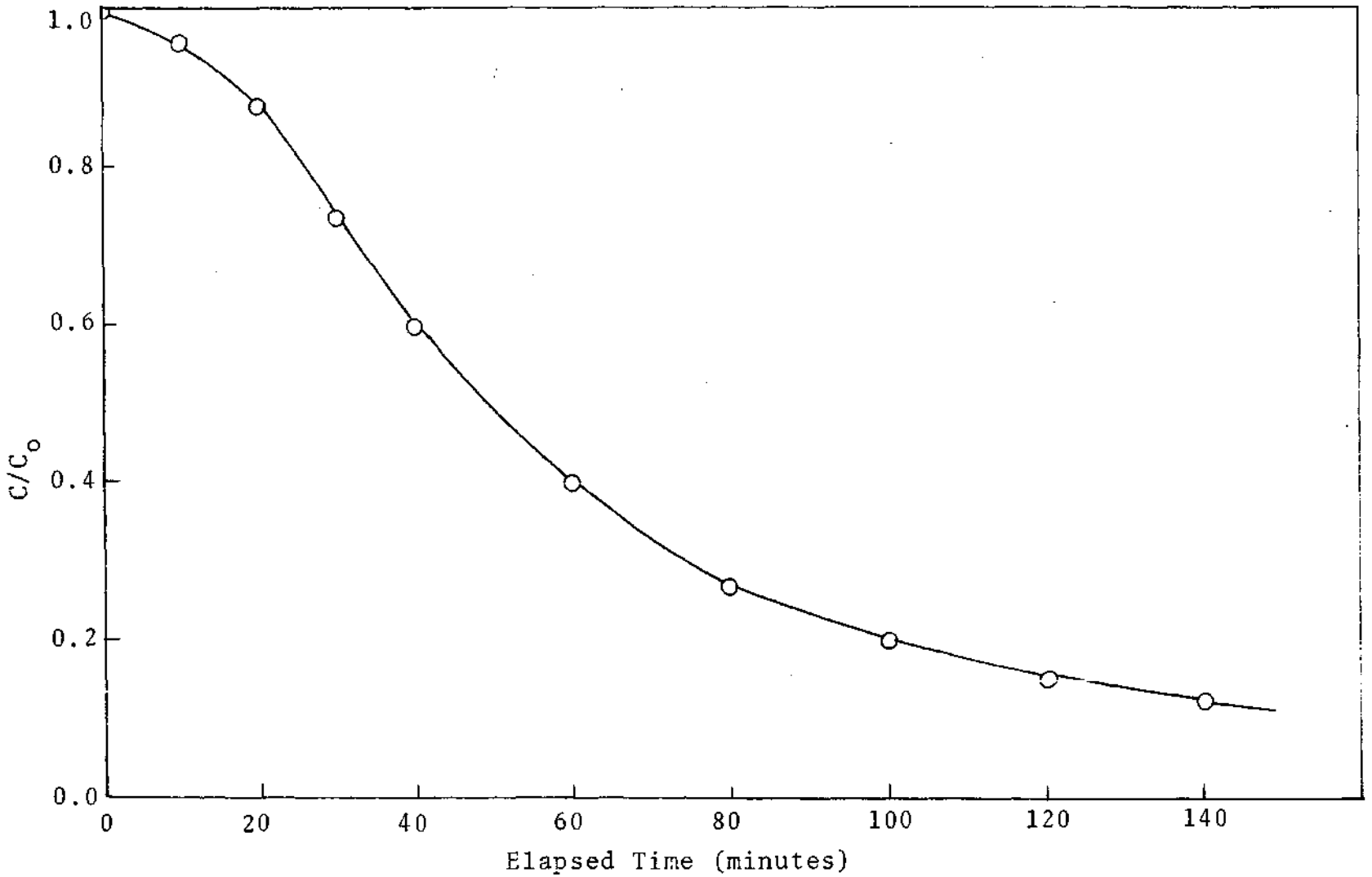

Figure 20. Desorption Curve for Test #1

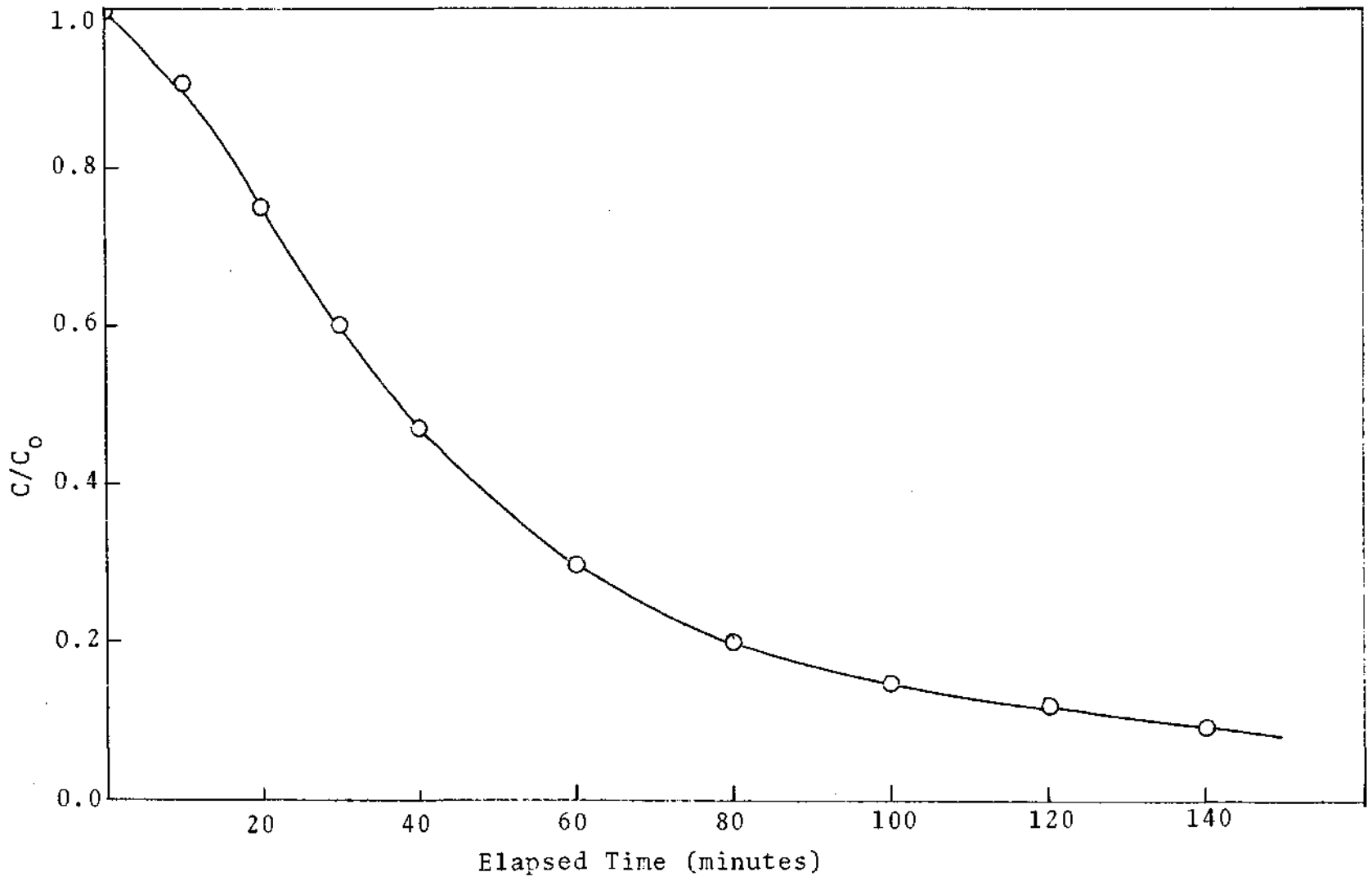

Figure 21. Desorption Curve for Test #5

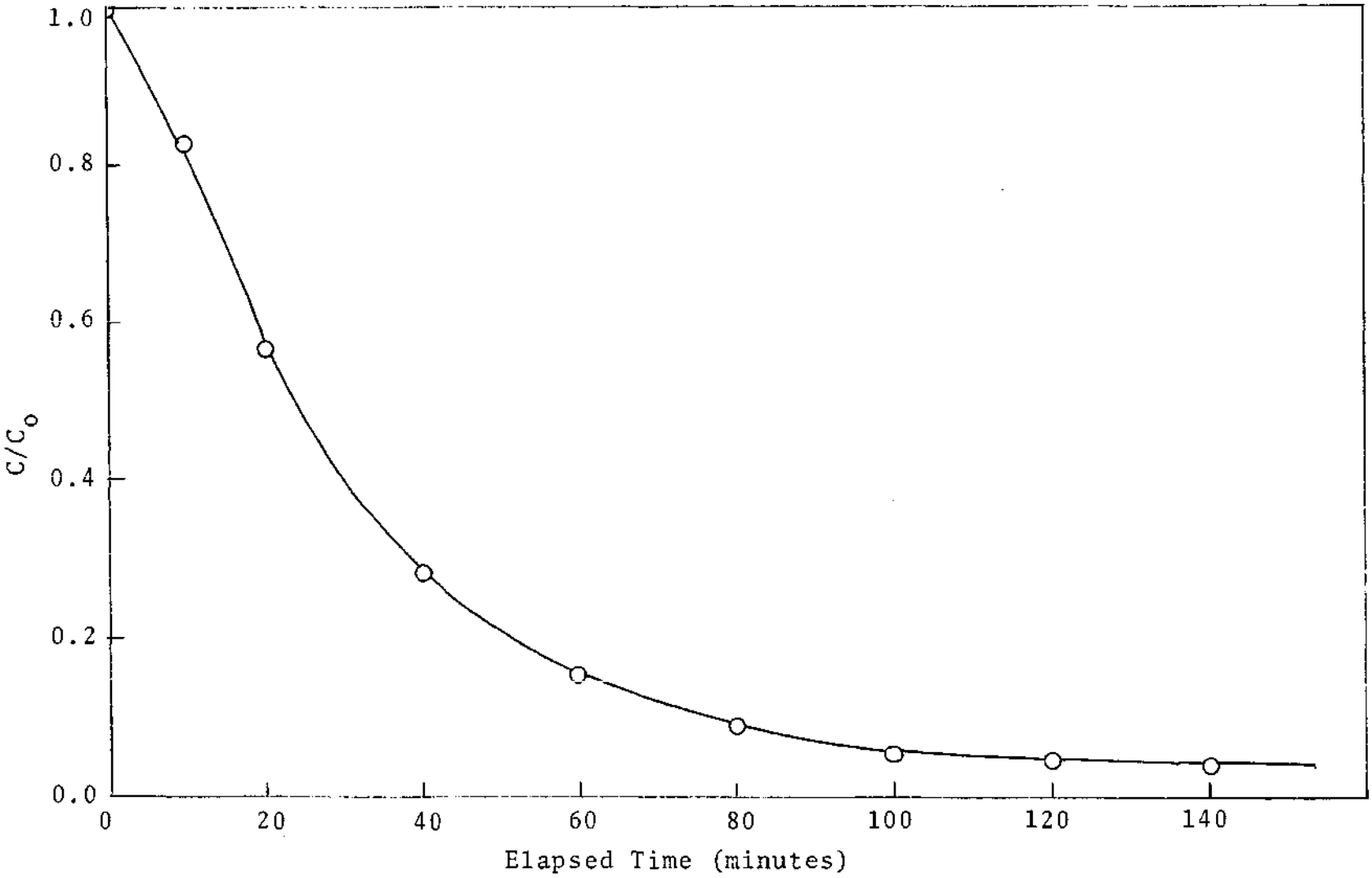

Figure 22. Desorption Curve for Test #9

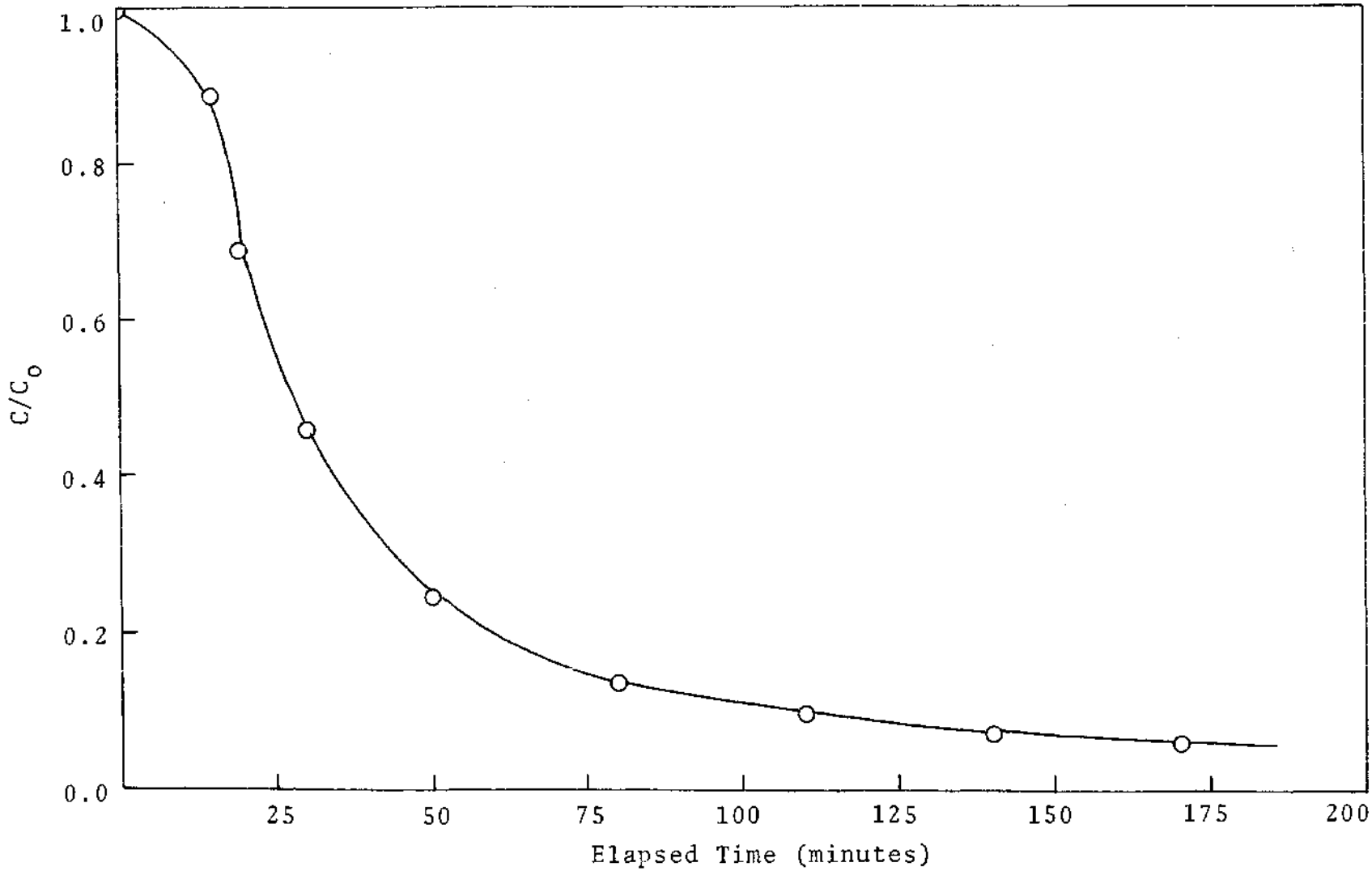

Figure 23. Desorption Curve for Test #2

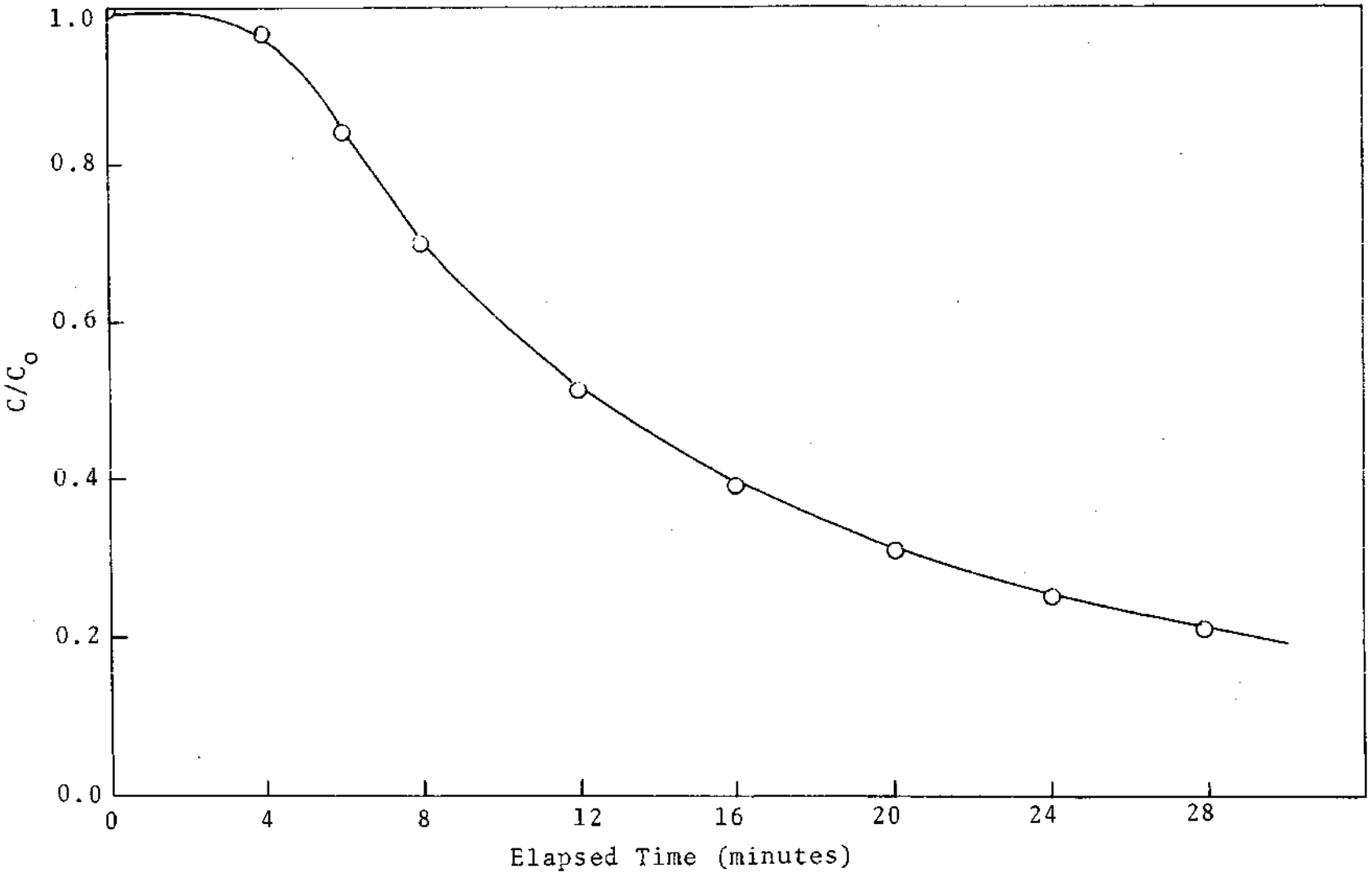

Figure 24. Desorption Curve for Test #6

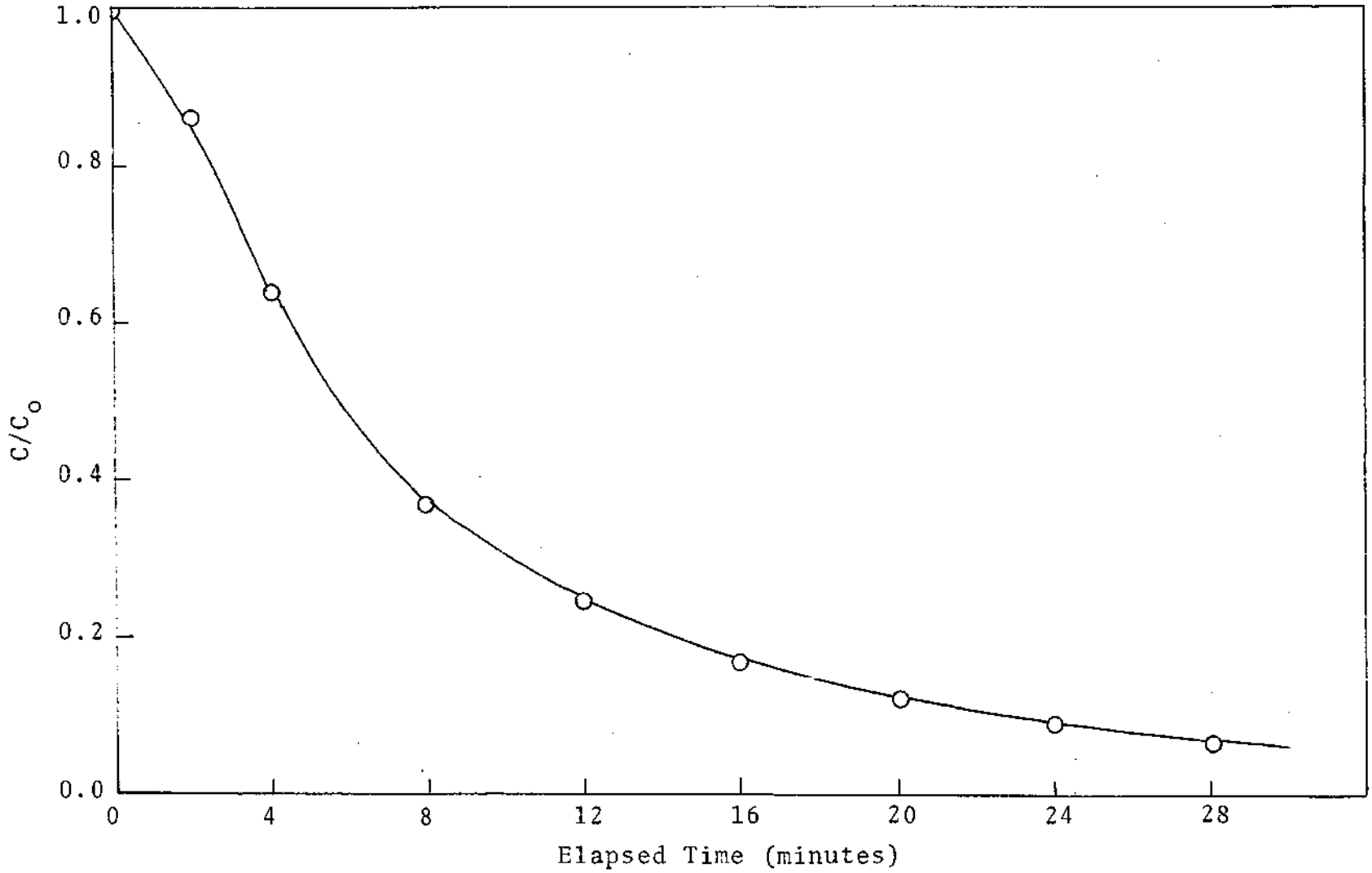

Figure 25. Desorption Curve for Test #10

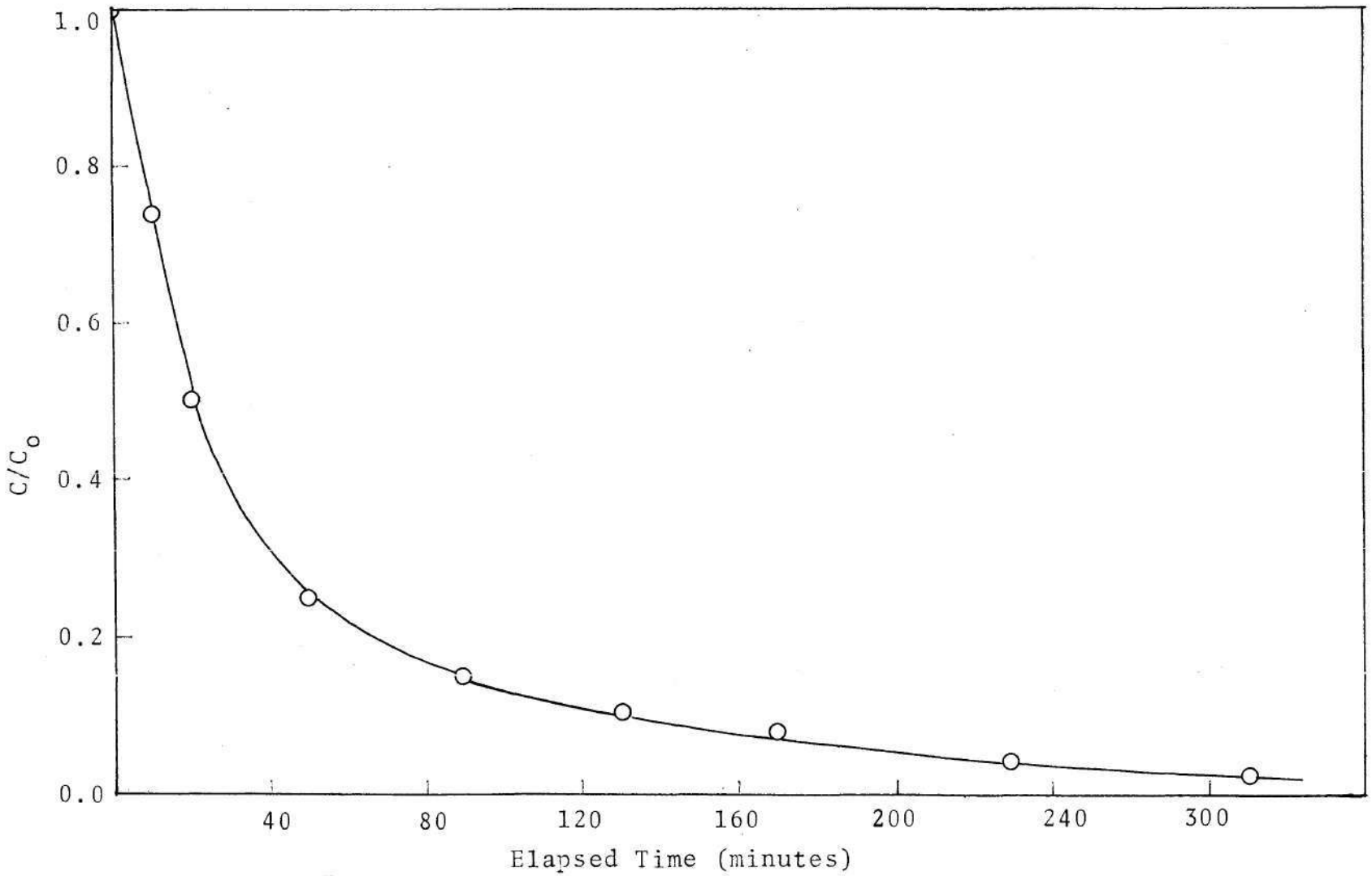

Figure 26. Desorption Curve for Test #3

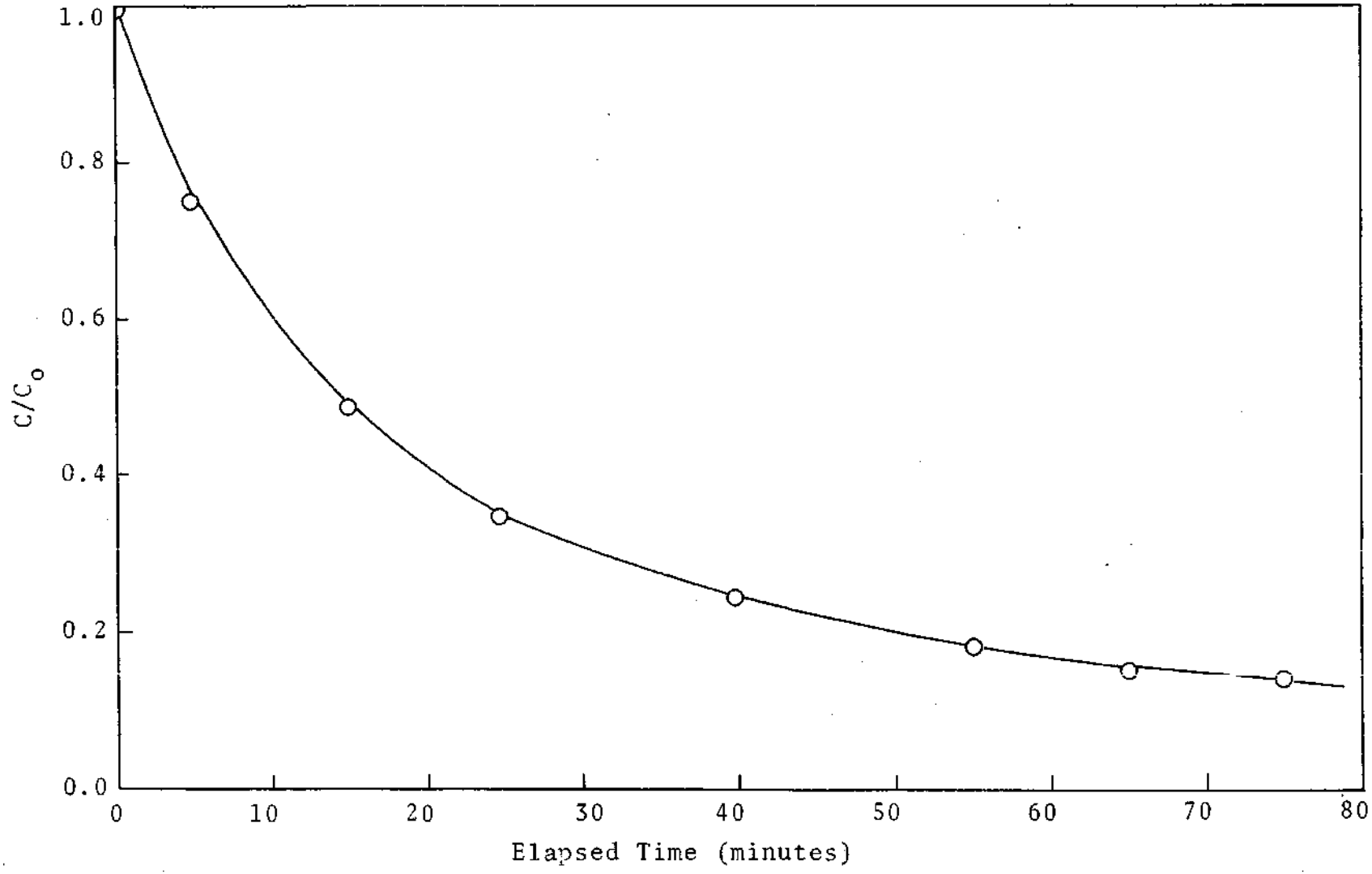

Figure 27. Desorption Curve for Test #7

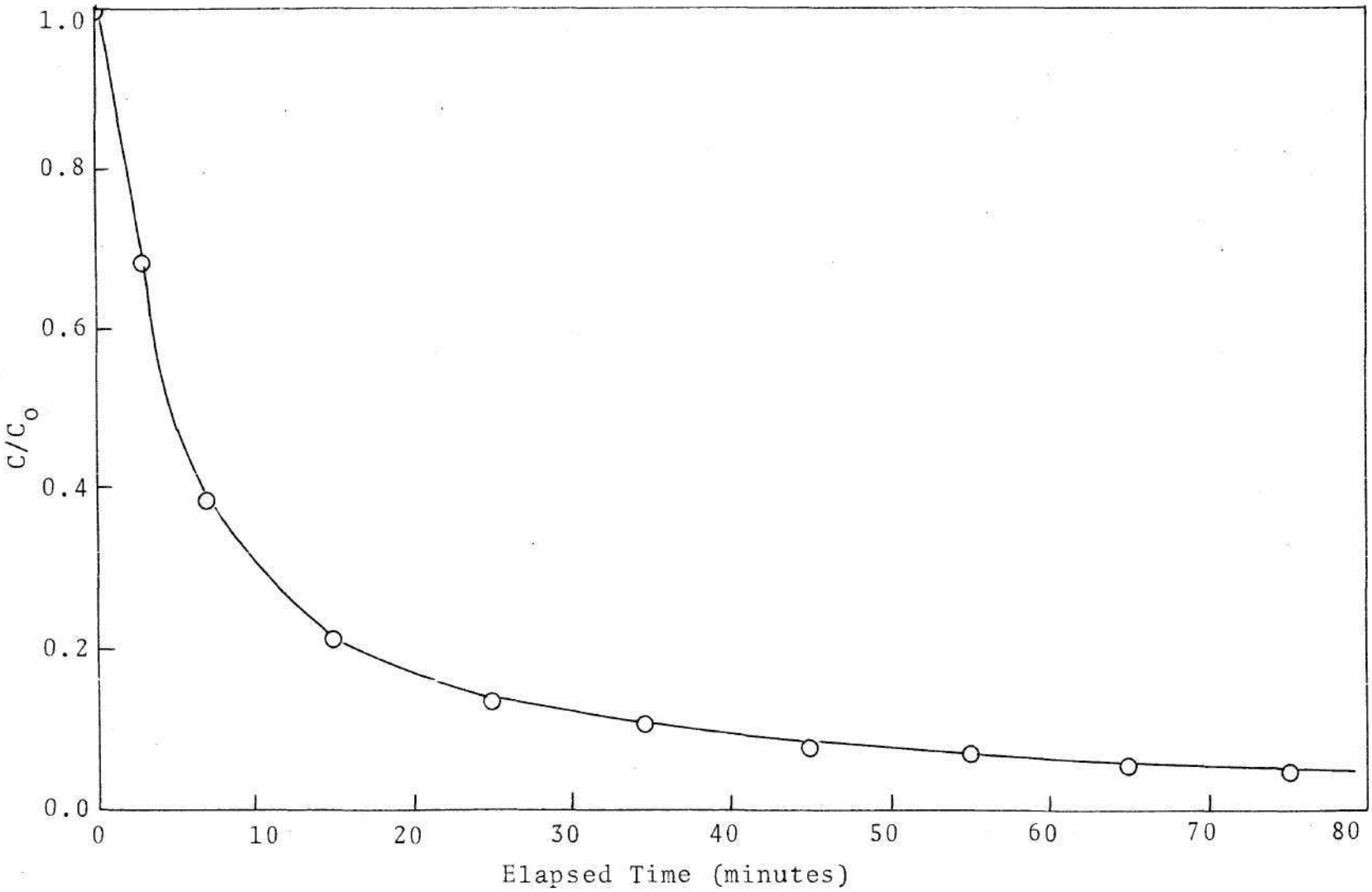

Figure 28. Desorption Curve for Test #11

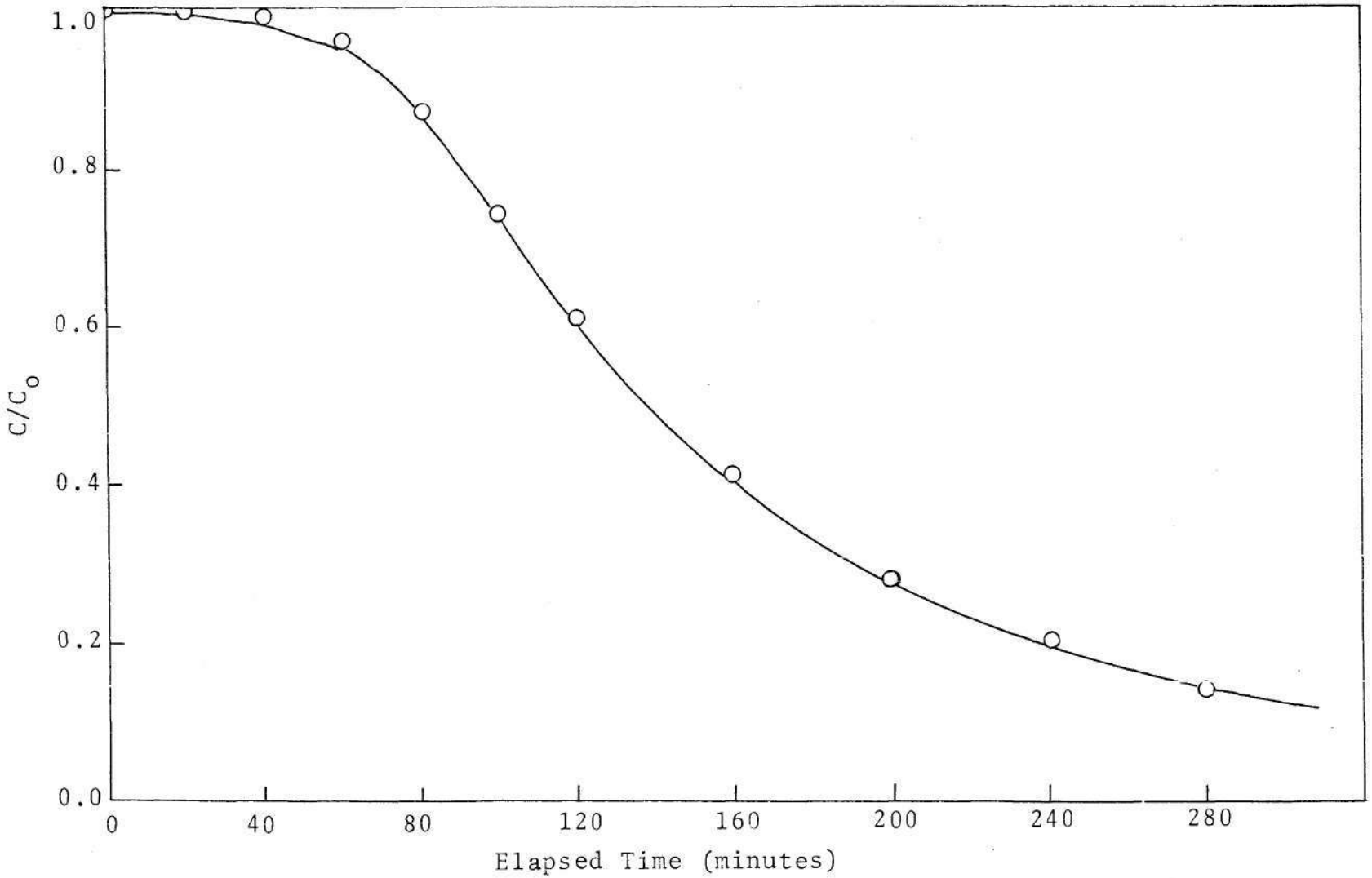

Figure 29. Desorption Curve for Test #4

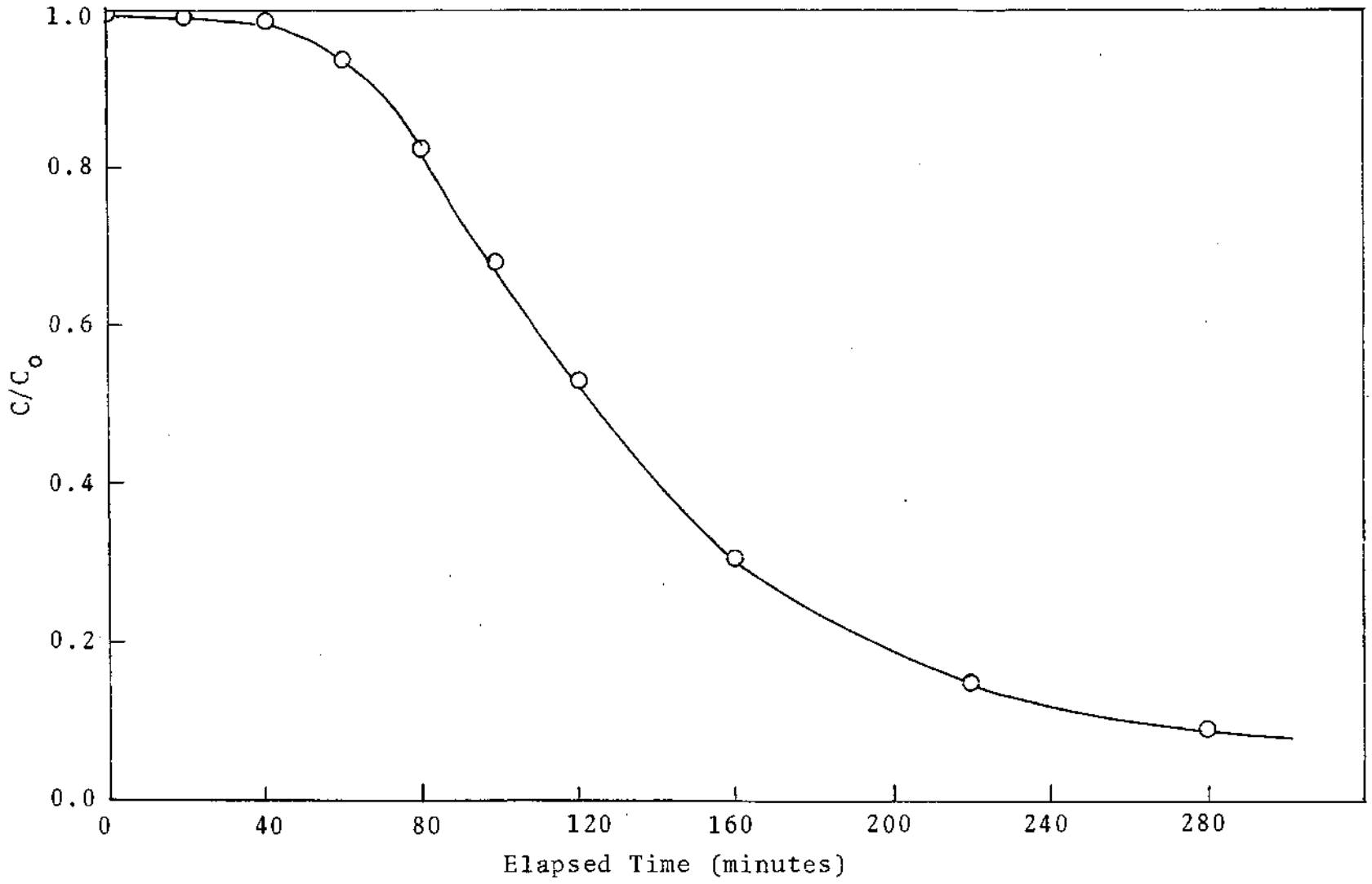

Figure 30. Desorption Curve for Test #8

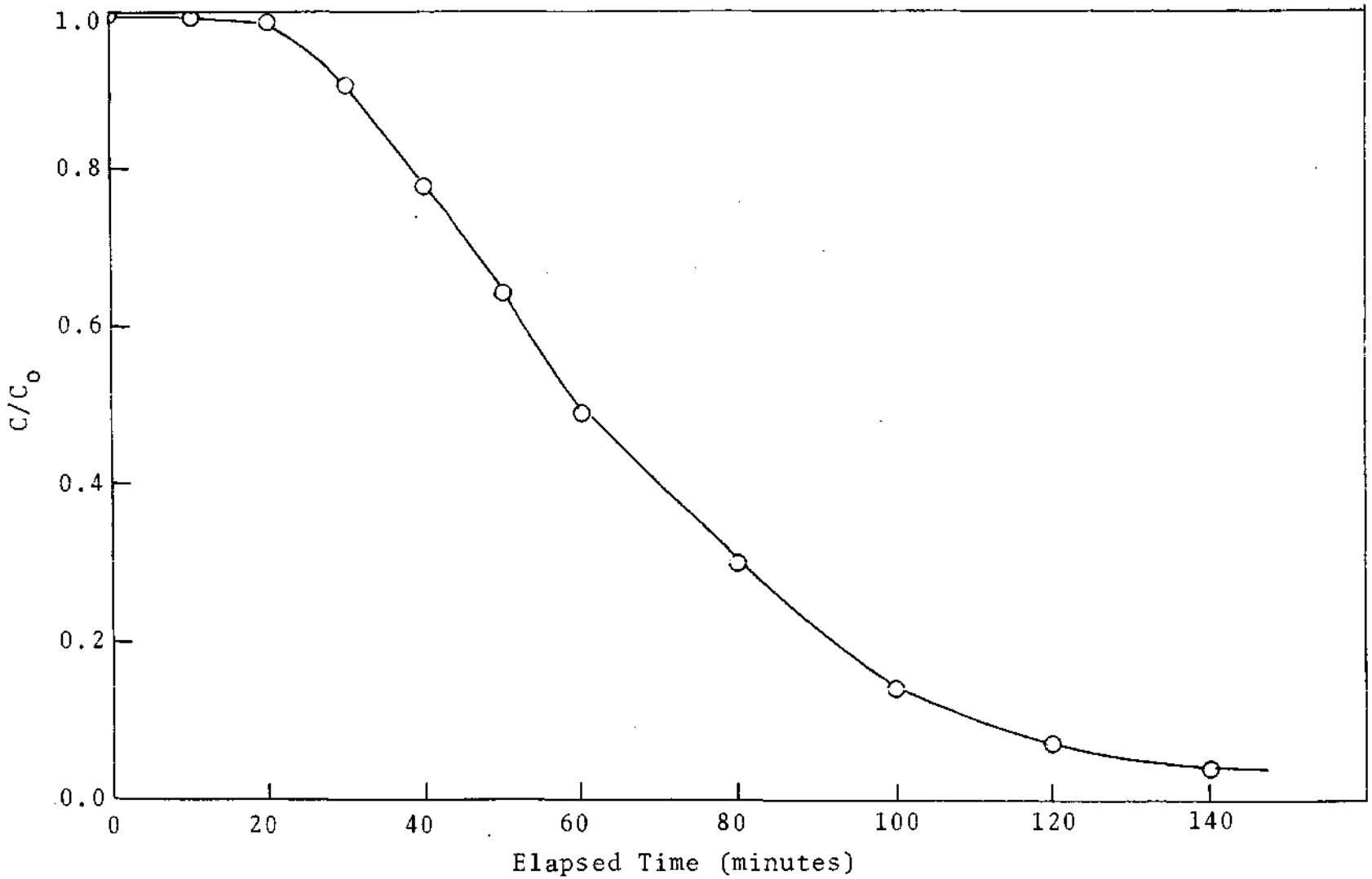

Figure 31. Desorption Curve for Test #12

CHAPTER V

DISCUSSION OF RESULTS

This investigation compared the adsorption of SO_2 on activated carbons derived from peanut hulls and waste rubber with general purpose commercially available activated carbons obtained from Westvaco and from Barnebey Cheneny. Rosen's general solution for fixed bed adsorption provided numerical estimates of the intraparticle diffusivities for the sulfur dioxide concentrations examined.

As seen from the tabulated values the diffusivities and equilibrium values are consistent with sulfur dioxide concentration and type of carbon. For example, the activated carbon derived from peanut hulls and raw rubber had intraparticle diffusivities greater than corresponding values for the commercial carbons for all three sulfur dioxide concentrations. A second example is that, in general, these intraparticle diffusivities increased in magnitude with increased adsorbate concentration.

Equilibrium constants, K_D, were also consistent with SO_2 concentration and type of carbon. As seen in Tables 1, 2, 3, and 4, carbon from peanut hulls adsorbed more sulfur dioxide per volume of adsorbent phase during tests run at 5005 and 11278 ppm SO_2. Westvaco carbon showed the second

highest overall capacity for adsorbed SO_2. Carbon produced from waste rubber and that supplied by Barnebey Cheney did not prove to have adsorption equilibrium values as large as the experimental carbons. In addition, it was observed that values of K_D decreased in magnitude with increased gas phase adsorbate concentration. This would imply two things: first, the available absorbing sights for sulfur dioxide molecules were becoming filled and second, the driving force needed for further adsorption was increasing.

From Figures 8 through 19 it is seen that the curve fits to Rosen's solution were good. However, in most cases these curves were steeper in slope at the upper and lower concentration limits. Rosen's solution was based on a number of assumptions: uniformly sized spherical particles, plug flow, negligible axial diffusion, isothermal operation, and the existence of a linear equilibrium isotherm. Except for the nonlinear adsorption isotherms, most of the above conditions were probably met experimentally.

The equilibrium isotherms for all activated carbon samples were favorable. The two commercial samples exhibited nearly linear relationships, with Westvaco's Nuchar being most linear. According to DeVault [11], favorable isotherms exhibit self-sharpening breakthrough curves with increased bed depth and time.

CHAPTER VI

CONCLUSIONS AND RECOMMENDATIONS

This study shows that peanut hulls and waste rubber can be used to produce high capacity activated carbon for sulfur dioxide adsorption at concentrations equal to or less than 11,000 ppm. From Table 1 the bulk densities, equilibrium coefficients, and intraparticle diffusivities indicate that peanut hull carbon gives the best overall results. Indications are that a fixed bed of this material would have lower total weight, hold a larger quantity of sulfur dioxide, and would become saturated with a very steep breakthrough curve. Activated carbon from waste rubber has the same type of weight advantages and exhibits steep breakthrough curves, but its capacity for adsorbing sulfur dioxide is not as great as activated carbon from peanut hulls.

Of the two commercially available activated carbons, Nuchar gave the best results. Table 1 indicates that Nuchar has a relatively large capacity for sulfur dioxide adsorption, but its breakthrough curve is not as steep as for peanut hull carbon. Due to its high bulk density a similar size adsorber unit would contain twice as much adsorbent by weight.

On the basis of this work, it is recommended that activated carbons derived from peanut hulls and waste rubber

be examined further to evaluate more fully their adsorptive properties of sulfur dioxide at different temperatures and pressures. In addition, the adsorption properties of these carbons should be evaluated with other gases at similar conditions to those used in this investigation.

APPENDICES

APPENDIX A

SAMPLE CALCULATIONS FOR TEST #9

z = bed height = 13.30 cm

A = cross sectional area of bed = 1.65 cm^2

ρ_p = particle density = 1.3949 gm/cm^3

w = weight of carbon bed = 6.5201 gm

Bed density $\rho_b = w/(Az)$

$= (6.5201)/[(1.65)(13.3)]$

$= 0.2971\ gm/cm^3$

Void fraction $\varepsilon = \dfrac{\rho_p - \rho_b}{\rho_p}$

$\varepsilon = (1.3949 - 0.2971)/(1.3949)$

$\varepsilon = 0.7870$

Void fraction/particle fraction:

$m = (\rho_p - \rho_b)/\rho_b$

$m = (1.3949 - 0.2971)/(0.2971)$

$m = 3.6950$

Sample calculation: Inlet concentration (Test #9)

Temperature = 532°R

Pressure = 745.0 mm Hg

Compressibility factor for SO_2 (f_{SO_2}) = 0.9816

Compressibility factor for N_2 (fN_2) = 1.000

Flowrate for SO_2 (F_{SO_2}) = 3.2827 cm^3/min

Flowrate for SO_2 and N_2 mixture (F_m) = 285.7143 cm^3/min

$$C_o' = (F_{SO_2} f_{SO_2})/(F_{mix} f_{mix})$$

$$C_o' = [(3.2827)(0.9816)]/[(285.7143)(1.0000)] \times 10^6$$

$$C_o' = 11278 \text{ ppm}$$

Sample calculation: Equilibrium coefficient (K_D)

$$T = 532.0°R = 295.56°K$$

$$P = 745 \text{ mm Hg} = 0.980 \text{ atm}$$

$$V = \frac{n\ R\ T}{P} = \frac{(1.00)(82.05)(295.56)}{(0.980)}$$

$$V = 24745.61 \text{ cm}^3/\text{gm-mole}$$

$$C_D = (mwt_{SO_2})(C_o)/(V)$$

$$C_D = (64.06 \frac{\text{gm}}{\text{gm-mole}})(1.1278 \times 10^{-2})/(24745.61 \text{ cm}^3)$$

$$C_D = 2.917 \times 10^{-5} \frac{\text{gm}}{\text{cm}^3}$$

$$G = (F)(\frac{491.67°R}{T})(\frac{P}{760.0 \text{ mm Hg}})$$

$$G = (285.71 \frac{\text{cm}^3}{\text{min}})(\frac{491.67}{532.00})(\frac{745}{760})$$

$$G = 258.839 \frac{\text{cm}^3}{\text{min}}$$

$$K_D = (\tau - \int \frac{C}{C_o} d\tau)(\rho_p)(G)/(w)$$

$$K_D = (72.73)(1.3949)(258.839)/(6.5201)$$

$$K_D = 4027$$

$$q = C_o K_D$$

$$q = (2.917 \times 10^{-5})(4027) = 1.175 \times 10^{-1} \frac{\text{gm } SO_2}{\text{cm}^3 \text{ carbon}}$$

Sample calculation: Intraparticle diffusion coefficient

$$\vec{v} = (F)/[(A_x)(\varepsilon)(60\ \frac{sec}{min})$$

$$\vec{v} = (258.839)/[(1.65)(0.7870)(60)]$$

$$\vec{v} = 3.32\ \frac{cm}{sec}$$

$$X = 705.5$$

$$D = [m\ \vec{v}\ b^2\ X]/[(3)K_D L]$$

$$D = (3.6950)(3.32)(0.02372)^2(705.5)/[(3)(4027)(13.3)]$$

$$D = 3.08 \times 10^{-5}\ \frac{cm^2}{sec}$$

APPENDIX B

EXPERIMENTAL DATA

Table 5. Experimental Data for Carbon from Peanut Hulls

Test #1		Test #5		Test #9	
Time (min)	C/C_o	Time (min)	C/C_o	Time (min)	C/C_o
132	0.000	106	0.020	82	0.022
134	0.266	107	0.069	83	0.052
136	0.537	108	0.131	84	0.267
138	0.666	109	0.204	85	0.586
140	0.764	110	0.283	86	0.707
146	0.860	112	0.429	87	0.782
154	0.899	114	0.552	90	0.885
160	0.918	115	0.619	95	0.947
170	0.945	117	0.718	100	0.982
180	0.960	120	0.798	105	0.994

Table 6. Experimental Adsorption Data for Carbon from Waste Rubber

Test #2		Test #6		Test #10	
Time (min)	C/C_o	Time (min)	C/C_o	Time (min)	C/C_o
42	0.004	13	0.000	7	0.000
44	0.229	14	0.168	8	0.140
46	0.476	15	0.635	9	0.782
48	0.573	16	0.780	10	0.874
50	0.627	17	0.836	11	0.918
56	0.745	20	0.895	12	0.941
60	0.774	25	0.936	13	0.953
70	0.822	30	0.946	14	0.976
80	0.846	40	0.968	17	0.994
90	0.865	50	0.976	20	0.999

Table 7. Experimental Adsorption Data for Carbon from Barnebey Cheney

Test #3		Test #7		Test #11	
Time (min)	C/C_o	Time (min)	C/C_o	Time (min)	C/C_o
130	0.000	130	0.014	60	0.023
132	0.033	133	0.128	62	0.037
134	0.119	135	0.240	64	0.103
138	0.211	138	0.412	65	0.150
142	0.423	140	0.506	66	0.217
146	0.538	143	0.635	68	0.359
150	0.643	146	0.735	70	0.514
160	0.865	150	0.836	72	0.680
170	0.922	160	0.968	74	0.812
180	0.956	170	0.996	80	0.999

Table 8. Experimental Adsorption Data for Carbon from Westvaco

Test #4		Test #8		Test #12	
Time (min)	C/C_o	Time (min)	C/C_o	Time (min)	C/C_o
20	0.000	6	0.080	7	0.018
30	0.245	7	0.190	8	0.036
40	0.442	8	0.290	9	0.138
50	0.547	9	0.381	10	0.277
60	0.619	10	0.450	11	0.393
70	0.665	15	0.653	13	0.553
80	0.706	20	0.754	15	0.667
100	0.754	25	0.818	17	0.734
120	0.791	30	0.856	22	0.848
140	0.815	50	0.957	30	0.947

APPENDIX C

CALIBRATION CURVES FOR INFRARED ANALYZER

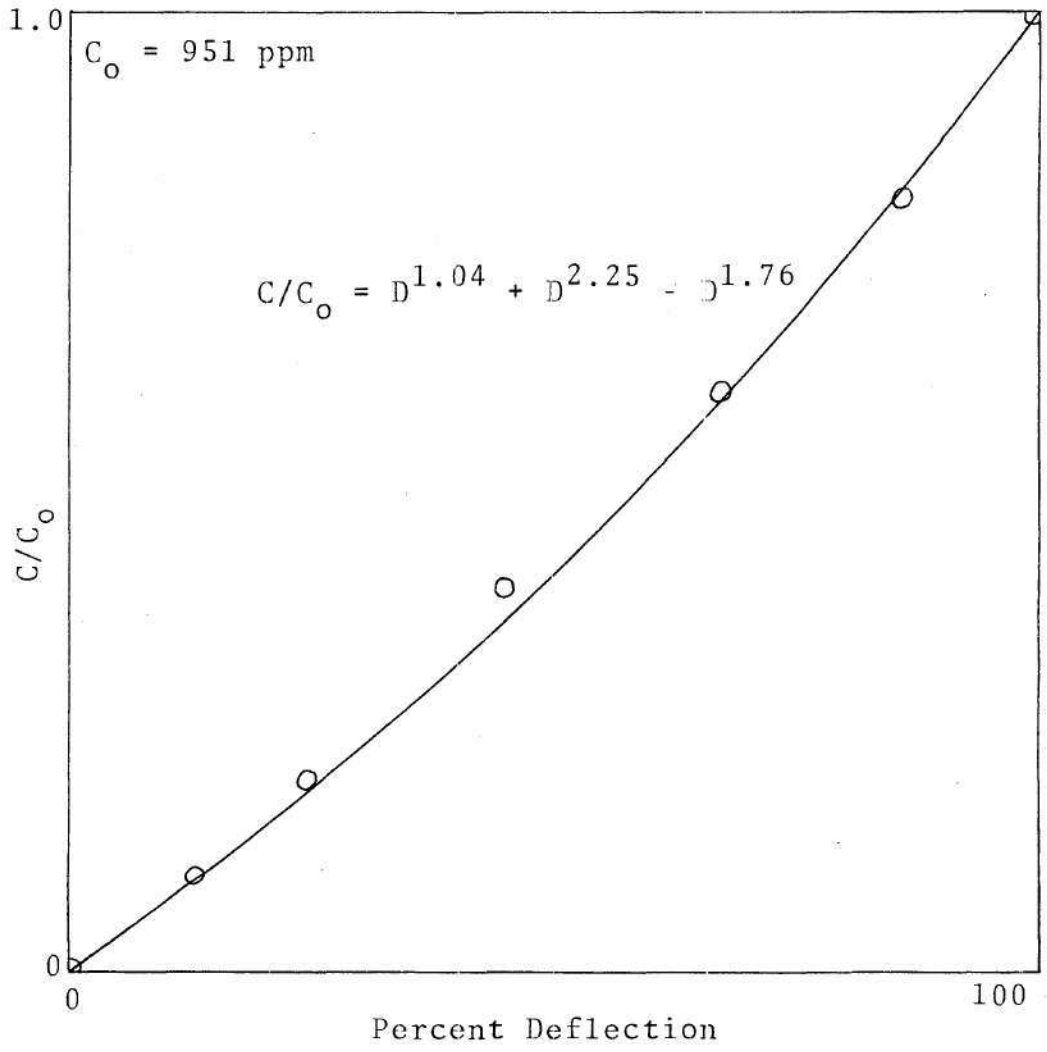

Figure 32. Calibration Curve for Infrared Analyzer at C_o = 951 ppm SO_2

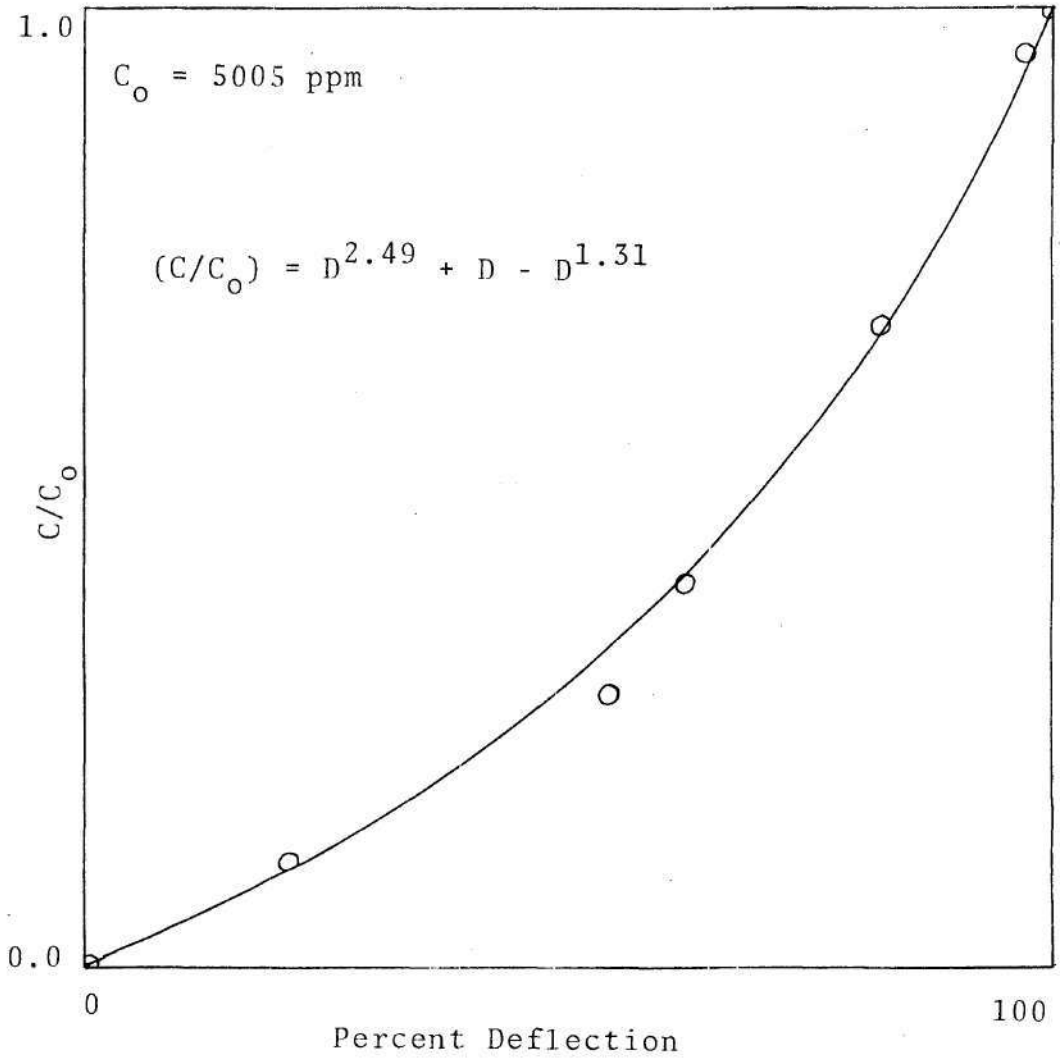

Figure 33. Calibration Curve for Infrared Analyzer at C_o = 5005 ppm SO_2

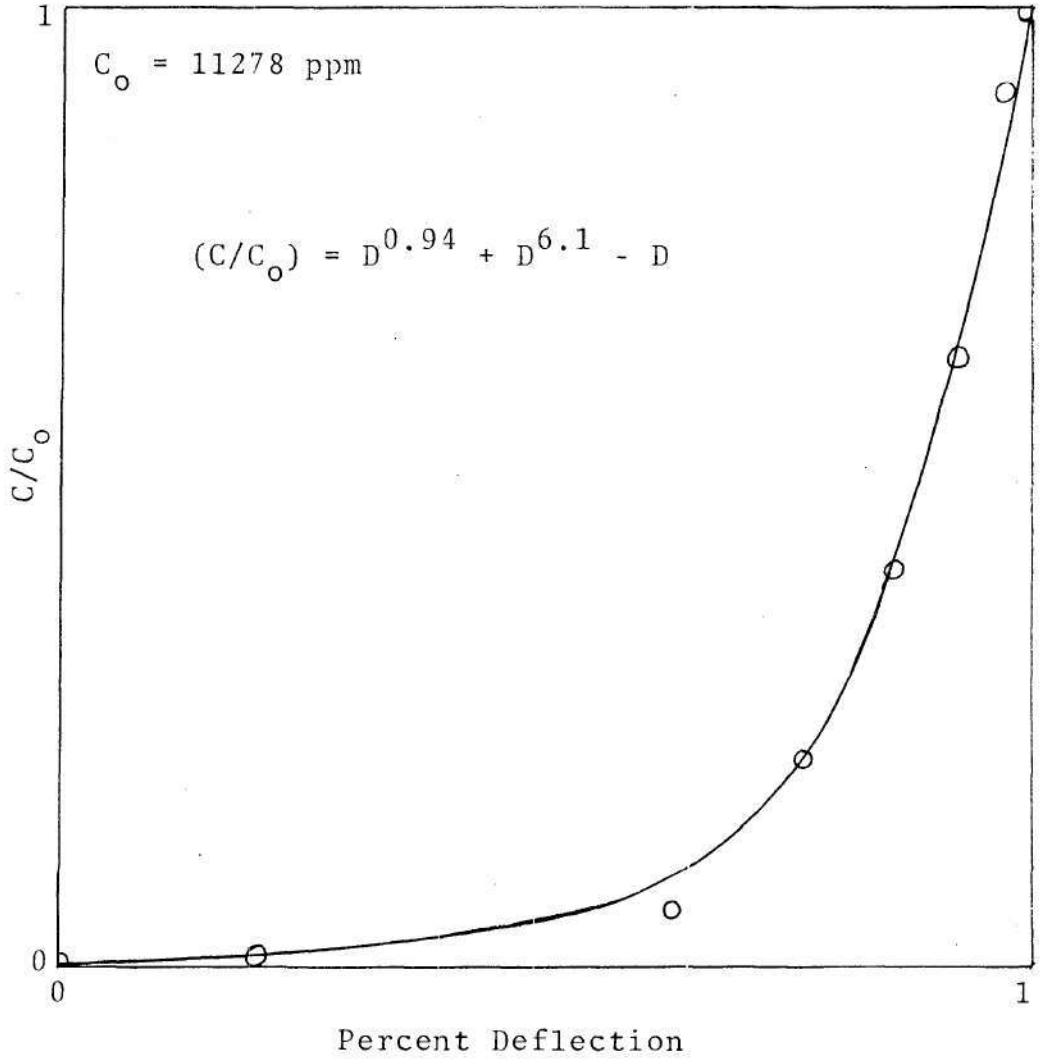

Figure 34. Calibration Curve for Infrared Analyzer at C_o = 11278 ppm SO_2

BIBLIOGRAPHY

1. Antonson, Carl R., "Kinetics of Ethane Adsorption on Molecular Sieves," M. S. Thesis, Northwestern University, (1966).

2. Barrer, R. M., Trans. Faraday Soc., 45, (1949), 368.

3. Beaton, R. H. and Furnas, C. C., Ind. Eng. Chem., 33, (1941), 1500.

4. Bischoff, W. F. and Habib, Y., "Processing: The FW-BF Dry Adsorption System," Chemical Engineering Progress, Vol. 71, No. 5 (1975), 59-60.

5. Bohart, G. D. and Adams, E. Q., J. Am. Chem. Soc., Vol. 42, (1920), 523.

6. Camp, David T., "Physical Adsorption of Argon and Nitrogen on Fixed Beds," Ph.D. Dissertation, Carnegie Institute of Technology (1963).

7. Campbell, Malcolm L., "Chemical Engineering Kinetics of Physical Adsorption," Ph.D. Dissertation, Carnegie Institute of Technology (1961), 6-8.

8. Carter, J. W., "Adsorption Drying of Gases," British Chemical Engineering, September (1960), 625-630.

9. Collins, J. J., "The LUB/Equilibrium Section Concept for Fixed-Bed Adsorption," in Physical Adsorption Processes and Principles, Canjar, Lawrence N., and Kostecki, John A., ed., Vol. 63 (1967), 31-35.

10. Colwell, C. J., M. S. Dissertation, Northwestern University, Evanston (1965).

11. DeVault, D. J., J. Am. Chem. Soc., Vol. 65 (1943), 532.

12. Furnas, C. C., Trans. AIChE, 24, (1930), 142.

13. Griffin, R. P. and J. S. Dranoff, AIChE J., 9, (1963), 283.

14. Habgood, H. W., Can. J. Chem., 36, (1958), 1384.

15. Juntgen, Harald and Peters, Werner, "Results of Recent Research in Waste Gas Desulfurization," Staub-Reinhalt Luft 28, No. 5, 1-6, March (1968).

16. Kostecki, John A., "The Kinetics of Physical Adsorption of Liquid Water from Benzene in Fixed-Bed Adsorbent Columns," Ph.D. Dissertation, Carnegie Institute of Technology (1964), 5-7.

17. Lee, Don R., "Activated Charcoal in Air Pollution Control," in Heating, Piping and Air Conditioning, April (1970), 76-79.

18. Masamune, S. and J. M. Smith, AIChE J., 10, (1964), 246.

19. Masamune, S. and J. M. Smith, AiChE J., 11, (1965), 41.

20. Perry, Robert H., Chilton, Cecil H., and Kirkpatrick, Sidney D., ed., Chemical Engineers' Handbook, 4th Ed., McGraw-Hill, Inc. (1963), 16-1 to 16-19.

21. Rosen, J. B., Eng. Design and Process Development, Vol. 46 (1954), 1590.

22. Rosen, J. B., J. Chem. Phys., Vol. 20 (1592), 387.

23. Stuart, Francis X. and Camp, David T., "Solution of the Fixed Bed Physical Adsorption Problem with Two Significant Rate Controlling Steps," in Gas Purification by Adsorption, Vol. 69 (1973).

24. Thomas, H. C., Ann. N. Y. Acad. of Sci., Vol. 49 (1948), 161-182.

25. Thomas, H. C., J. Am. Chem. Soc., Vol. 66 (1944), 1664.

26. Treybal, Robert E., ed., Mass-Transfer, first edition, McGraw-Hill, Inc., New York (1955), 499.

27. Treybal, Robert E., ed., Mass-Transfer, second edition, McGraw-Hill, Inc., New York (1968), Chapter 11.

28. Vassiliou, B. and J. S. Dranoff, AIChE J., 8, (1962), 248.

29. Vermuelen, T., "Separation by Adsorption Methods," in Advances in Chemical Engineering, Vol. 2, Drew, T. B., and Hoopes, J. W., Jr., New York, Academic Press (1958), 165.

30. Walter, J. E., J. Chem. Phys., Vol. 13 (1945), 229.